CANADIAN THESES ON MICROFICHE

THÈSES CANADIENNES SUR MICROFICHE

National Library of Canada
Collections Development Branch

Canadian Theses on
Microfiche Service

Ottawa, Canada
K1A 0N4

Bibliothèque nationale du Canada
Direction du développement des collections

Service des thèses canadiennes
sur microfiche

NOTICE

The quality of this microfiche is heavily dependent upon the quality of the original thesis submitted for microfilming. Every effort has been made to ensure the highest quality of reproduction possible.

If pages are missing, contact the university which granted the degree.

Some pages may have indistinct print especially if the original pages were typed with a poor typewriter ribbon or if the university sent us an inferior photocopy.

Previously copyrighted materials (journal articles, published tests, etc.) are not filmed.

Reproduction in full or in part of this film is governed by the Canadian Copyright Act, R.S.C. 1970, c. C-30. Please read the authorization forms which accompany this thesis.

AVIS

La qualité de cette microfiche dépend grandement de la qualité de la thèse soumise au microfilmage. Nous avons tout fait pour assurer une qualité supérieure de reproduction.

S'il manque des pages, veuillez communiquer avec l'université qui a conféré le grade.

La qualité d'impression de certaines pages peut laisser à désirer, surtout si les pages originales ont été dactylographiées à l'aide d'un ruban usé ou si l'université nous a fait parvenir une photocopie de qualité inférieure.

Les documents qui font déjà l'objet d'un droit d'auteur (articles de revue, examens publiés, etc.) ne sont pas microfilmés.

La reproduction, même partielle, de ce microfilm est soumise à la Loi canadienne sur le droit d'auteur, SRC 1970, c. C-30. Veuillez prendre connaissance des formules d'autorisation qui accompagnent cette thèse.

THIS DISSERTATION
HAS BEEN MICROFILMED
EXACTLY AS RECEIVED

LA THÈSE A ÉTÉ
MICROFILMÉE TELLE QUE
NOUS L'AVONS REÇUE

Canada

NL 339 (r. 85/09)

Solubility Measurement in Supercritical Fluids by Chromatography

by

Michael Robert Margerum

A thesis
presented to the University of Ottawa
in fulfillment of the
thesis requirement for the degree of
Master of Applied Science
in
Chemical Engineering

Department of Chemical Engineering
University of Ottawa

Ottawa, Ontario, 1985

ACKNOWLEDGMENTS

I would like to express my sincere gratitude to my research director, Dr. B. C.-Y. Lu, Professor of Chemical Engineering at the University of Ottawa, for his support and for the opportunity to work on this project.

I would also like to thank Dr. K. Ohgaki, Assistant Professor of Chemical Engineering at Osaka University, for his invaluable assistance and advice.

I have also appreciated the help of the technical staff of the Department of Chemical Engineering of the University of Ottawa. My thanks go out to Mr. J. Gasperetti, Mr. D. Lefebvre and Mr. A. Bonaldo.

A special thank-you goes to Miss Amy Lui for her support and for her aid in the graphics of this thesis. I am also grateful to Mr. J.-M. Yu for his help on the word-processor.

Finally, I would like to acknowledge the financial support of the Natural Sciences and Engineering Research Council of Canada.

ABSTRACT

A new method for the measurement of solubilities in supercritical fluids is developed. This method uses a supercritical fluid chromatograph to directly sample and analyze the fluid phase. Equilibrium between the solid and fluid phases is achieved using either a flow method or a static displacement method. The flow method is shown to give more precise results.

A calibration equation relating solubility to pure solvent compressibility factors and solute peak areas as measured on the chromatograph is developed. A calibration factor for naphthalene is determined by comparing experimental results to previous data for the naphthalene-carbon dioxide system. Calibration factors for other solutes are easily determined from that for naphthalene. The calibration factors are shown to be independent of the solvent used.

Solubility measurements for the naphthalene-carbon dioxide, anthracene-carbon dioxide, biphenyl-carbon dioxide and anthracene-ethylene systems are found to compare well with those of previous workers. Except for the biphenyl-carbon dioxide system, the results are well correlated by the Soave-Redlich-Kwong equation of state with a one-parameter random mixing rule.

NOMENCLATURE

- a(T), b : Soave-Redlich Kwong equation constants.
- A,B : Alternate forms for the above constants.
- b : carbon dioxide equation constants.
- B : ethylene equation constants.
- c : calibration factor, for T in K and P in Pa.
- c : ratio of calibration factors.
- f : fugacity.
- f : proportionality constant.
- G : molar Gibbs free energy.
- k : binary interaction coefficient.
- m : mass.
- MW : molecular weight.
- n : number of moles.
- P : pressure.
- R : gas constant.
- s : peak area.
- S : molar entropy.
- T : temperature.
- v : molar volume.
- V : volume.
- y : mole fraction.
- Z : compressibility factor.

- ϕ : fugacity coefficient.
- μ : chemical potential.
- ρ : density.
- ω : acentric factor.

Superscripts:

- S : solid.
- F : fluid.
- o : reference state.
- SAT : saturated state.
- * : expected value.

Subscripts

- # : refers to a component.
- i,j : refer to components.
- c : critical property.
- r : reduced property.

TABLE OF CONTENTS

FIGURES

TABLES

Chapter I

INTRODUCTION

Recently there has been much interest in the field of supercritical fluid extraction. An important research aspect of this field is the measurement of solubilities in supercritical fluids. In this work, an improved method of solubility measurement using supercritical fluid chromatography is developed.

This section serves as a general introduction to supercritical fluid extraction and its applications. Current research needs are identified, and research objectives are outlined.

1.1 Supercritical Fluids

The phase behaviour of a pure substance can be represented on a plot of pressure (P) versus temperature (T). Figure 1 is a typical P-T projection of a pure substance. When one of the lines separating the phases on this diagram is crossed, an obvious phase change occurs. Note that the demarcation line between the gas and liquid regions ends at the critical point. In the region beyond the critical point, no clear distinction can be made between the gas and liquid phases. Therefore, the term supercritical fluid is applied to this region.

A supercritical fluid is an intermediate between a liquid and a gas. Its properties are therefore intermediate between those of a liquid and a gas. Table 1 compares typical values of density, viscosity and diffusion coefficient.

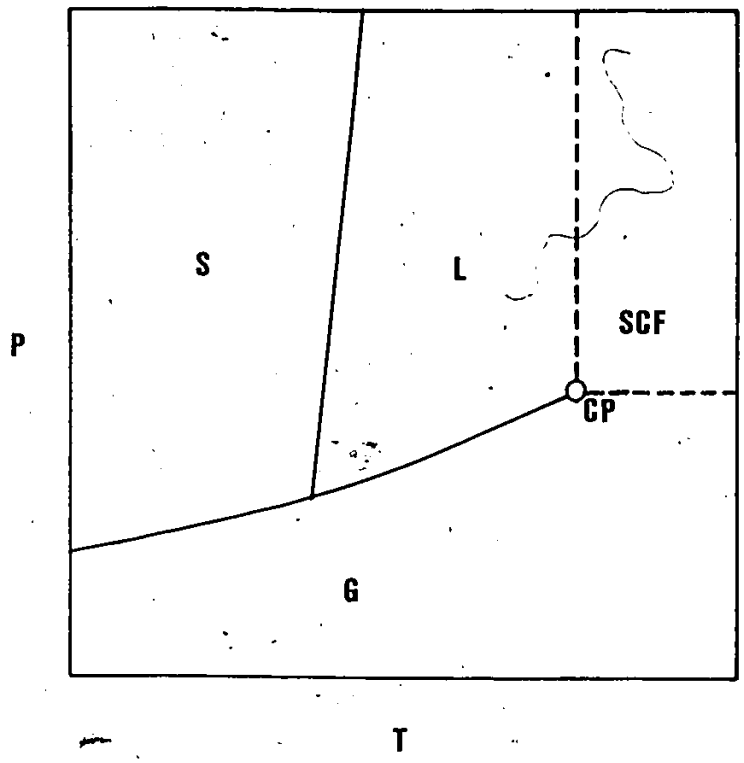

Figure 1: P-T Projection for a Pure Substance. S: solid. L: liquid. G: gas. SCF: supercritical fluid. CP: critical point.

A supercritical fluid has a density approaching that of a liquid. Solubilities are therefore much higher in a supercritical fluid than in a gas. Non-ideal interactions in the dense supercritical fluid increase the solubility still further, as first discovered by Hannay and Hogarth in 1890 [1]. Even low volatility substances are readily dissolved by a supercritical fluid. Solubilities are often thousands of times greater than in the ideal case.

The viscosity of a supercritical fluid is less than that of a liquid. In addition, the diffusivities of substances in a supercritical fluid are greater than in a liquid. There is thus less resistance to mass transfer than in a liquid.

These characteristics make supercritical fluids desirable solvents in separation processes. Separation processes using supercritical fluids as solvents are termed supercritical fluid extraction.

Table 1: Properties of a Supercritical Fluid, a Gas and a Liquid. The supercritical fluid is carbon dioxide near its critical point.

Fluid	Density g/mL	Viscosity cp	Diffusion coefficient cm^2/g
Supercritical fluid	0.7	0.01	0.01
Gas	0.001	0.001	0.1
Liquid	1	0.1	0.00001

1.2 Supercritical Fluid Extraction

Supercritical fluid extraction has received much attention in recent years because it exhibits several desirable characteristics. It often has significant advantages over other phase equilibrium separations, such as distillation or liquid extraction.

The solvent power of a supercritical fluid is determined by its density. The density is in turn strongly affected by temperature and pressure. Figure 2 shows typical solubilities of a low volatility substance in a supercritical fluid as a function of temperature and pressure. Near the critical point, isothermal compression causes a very large increase in solubility. In addition, isobaric heating near the critical point causes a large decrease in solubility. This results in several advantages for supercritical fluid extraction compared to distillation and liquid extraction. The recovery of solvent is straightforward and complete, unlike liquid extraction. Simple isothermal decompression or isobaric heating suffices to recover the solvent. It can then be compressed or heated and recycled. Since the solubilities of individual components may vary strongly from one another, it is also possible to fractionate the product by controlling the conditions of solvent recovery. If the solubilities change strongly enough with density, then supercritical fluid extraction uses considerably less energy than distillation.

Another advantage of supercritical fluid extraction is that a large number of variables can be manipulated to significantly affect separation. As mentioned above, temperature and pressure strongly affect solubility. The significant interactions between solvent and solute in

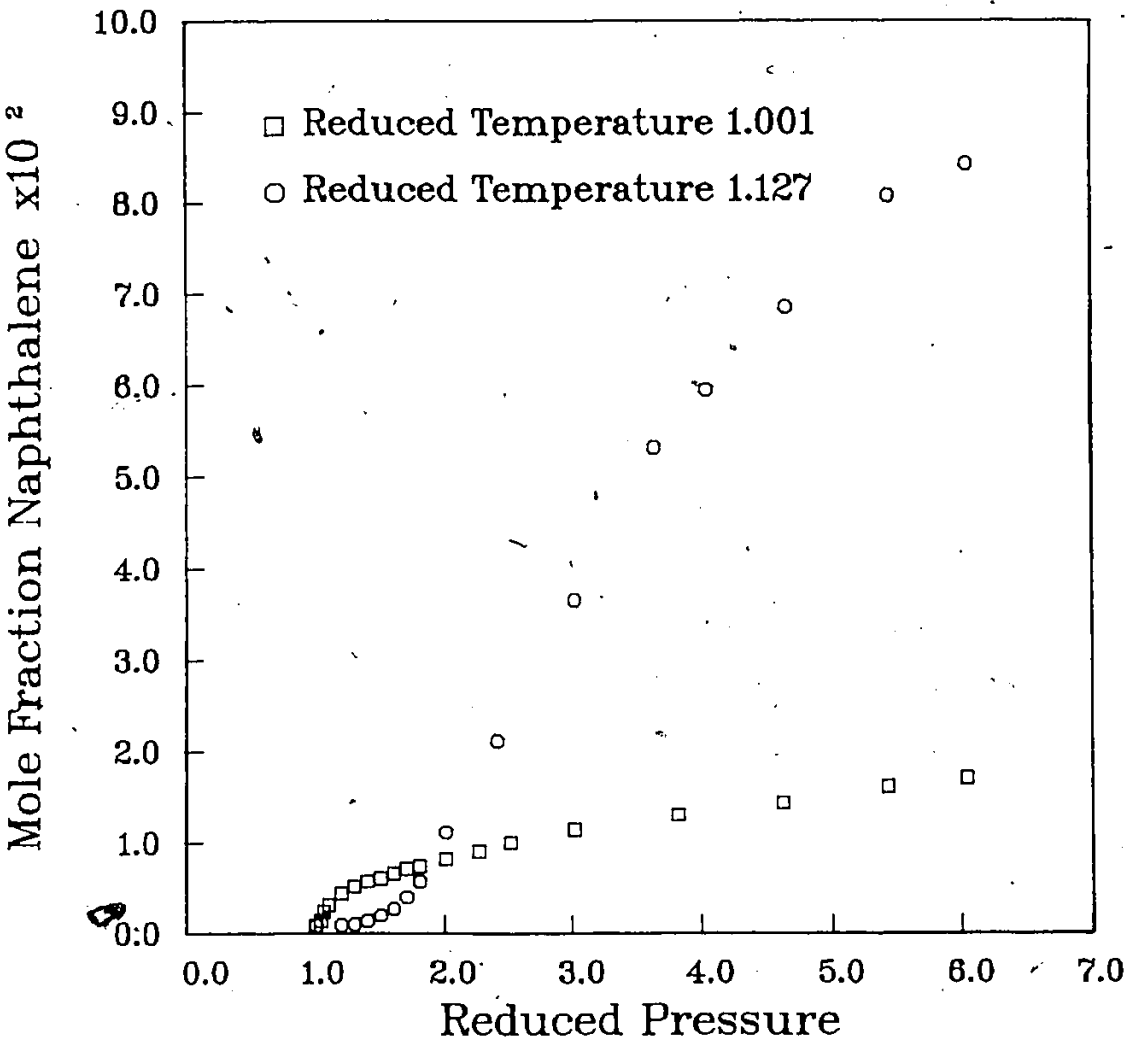

Figure 2: Solubility of Naphthalene in Supercritical Ethylene. The data is from Tsekhanskaya et al. [2].

the dense supercritical fluid make the choice of solvent important. The addition of a small amount of another substance, often termed an entrainer, can also have a significant effect.

Supercritical fluid extraction uses solvents such as carbon dioxide, ethylene and propane. There are several advantages in using such substances. They are inexpensive, especially compared to some solvents used in liquid extraction. They are non-toxic and can be completely recovered from the product. This is particularly important in the food industry. Finally, their low critical temperatures (for example, the critical temperature of carbon dioxide is 304.2 K) result in low operating temperatures, thus avoiding damage to thermally labile substances.

The major disadvantage of supercritical fluid extraction is high equipment cost. Expensive high pressure equipment is required to attain supercritical conditions (for example, the critical pressure of carbon dioxide is 7.38 MPa). In addition, lubricating oils and conventional sealing materials tend to dissolve in supercritical fluids. Specialized pumps and seals are therefore required, which further add to the expense . Because of its high cost, supercritical fluid extraction is usually considered only where distillation or liquid extraction have significant disadvantages.

1.3 Supercritical Fluid Applications

Several industrial processes have been developed which use supercritical fluid extraction. A few processes have been commercialized and are in production. In addition, supercritical fluids have found some use in the field of chromatography. Some of the applications of supercritical fluids are described below.

Supercritical fluid extraction has shown promise in the field of coal liquefaction. Conventional processes use high temperature solvent extraction. This has the disadvantage that desirable light components in the coal polymerize at the high operating temperatures used. Research at Britain's National Coal Board [3] has shown that supercritical fluids such as toluene can be used to extract the light components of coal. The operating temperatures are low enough to prevent polymerization.

The Kerr-McGee corporation has developed the Residual Oil Supercritical Extraction (ROSE) process for the fractionation of petroleum residues [4]. In this process, supercritical pentane extracts heavy oils from petroleum residues, leaving behind asphaltenes and heavy metal contaminants. The extract is separated by stagewise isobaric heating into resin and light oil fractions. The utility costs for the ROSE process are as much as 50 % less than those for conventional steam distillation. In addition, the removal of contaminants during the extraction stage allows the products to be processed without further treatment.

Kerr-McGee has developed a variant of the ROSE process known as Critical Solvent Deashing [5]. This process uses a supercritical solvent to separate ash from coal liquids. Isobaric heating is used to recover the deashed product. An expensive filtering step is therefore not needed.

Several other applications of supercritical fluids in the energy field have been explored [6]. These include enhanced oil recovery by miscible displacement with supercritical carbon dioxide, the extraction

of bitumen from tar sand and oil shale, and the fractionation of various fossil materials.

Supercritical fluid extraction has many applications in the food industry, because it offers an alternative to the toxic solvents often used in liquid extraction processes. Carbon dioxide is a popular solvent, because it is plentiful, inexpensive and non-reactive. One example is in the decaffeination of coffee beans. Hag AG in West Germany has developed a process using supercritical carbon dioxide to extract caffeine from green coffee beans [7]. The caffeine is recovered by decompression, water scrubbing or adsorption onto activated carbon. Supercritical carbon dioxide is also used in the extraction of hop resins from hops. Several hops extraction plants have been built in Germany [8].

Many other applications of supercritical fluid extraction in the food and chemical industries have been proposed [6]. Various fragile drugs can be purified without damage. Oils, flavor components and aroma components can be extracted from various natural products. Supercritical fluids extract organics from dilute aqueous solutions, often with considerable energy savings compared to distillation. Activated carbon can be regenerated by removing adsorbed substances with a supercritical fluid.

An important non-industrial use of supercritical fluids is the field of chromatography [9]. A supercritical fluid is a desirable mobile phase in a chromatograph. Since mass transfer is faster in a supercritical fluid than in a liquid, a supercritical fluid chromatograph demonstrates higher separation efficiencies in comparison to a liquid

chromatograph. Gas chromatography requires that the compounds being analyzed be vaporized at relatively low pressures, which is impractical in the case of thermally unstable or low volatility substances. The analysis of mixtures containing such compounds is possible with supercritical fluid chromatography, since operating temperatures are low, and low volatility substances are readily dissolved in a supercritical fluid.

1.4 Research Objectives

From the previous section it is apparent that much research has been made on the industrial applications of supercritical fluid extraction. Nevertheless, only the ROSE process, hops extraction and Hag AG's decaffeination process are in limited commercial use. Part of the reason for the slow acceptance of supercritical fluids extraction by industry is the high equipment cost mentioned above. A more fundamental problem was pointed out by Basta and McQueen [10]:

> Perhaps the key hurdle is that too little is known about the thermodynamics of supercritical systems.

Supercritical fluid systems have very complex solubility charts and phase diagrams, especially for multicomponent systems. This makes gathering, understanding and correlating data difficult.

One reason little is known about the thermodynamics of supercritical fluid systems is that the gathering of data is slow and tedious. The measurement of solubilities in the supercritical phase is an example of this. Existing methods are generally restricted to simple binary systems, may require considerable time and effort, and involve complex and/or indirect sampling and analysis methods.

Gas chromatography might seem to be a useful method of analysis. It offers the advantages of rapid and simple composition measurement, and it is not restricted to binary systems. However, many of the solutes in supercritical fluid systems are thermally fragile or have low volatility. As mentioned above, supercritical fluid chromatography is more suitable for the analysis of mixtures containing such substances. Randall [11] has commented that another advantage is that a sample being analyzed remains at supercritical conditions.

The objective of this work is to develop a fast, simple method of measuring solubilities in supercritical fluids, through the use of supercritical fluid chromatography. The method is developed and tested using well defined binary systems. The supercritical fluids used are carbon dioxide and ethylene, while the solutes are low volatility solids, namely naphthalene, anthracene and biphenyl. These systems are chosen for several reasons. First of all, their phase behavior is well understood. If a region of solid-fluid equilibrium is studied, then only the fluid phase needs to be analyzed, since the solid can be assumed to be pure. The solubility results can be compared with existing data, thus allowing evaluation of the method. Finally, simplifications resulting from the assumption of a pure solid phase permit the results to be easily correlated.

Chapter II

BACKGROUND

It has been pointed out in the Introduction that in order to properly understand and interpret supercritical fluid phenomena, the phase behaviour of supercritical fluid systems must be known. The types of phase behavior that occur in binary systems are therefore examined below, with particular attention to highly asymmetric solid-fluid systems. The work that has been done in the measurement of solid solubilities in supercritical fluids is reviewed.

2.1 Supercritical Fluid Phase Behavior

Supercritical fluid systems have complex phase behavior, especially as the number of components is increased. An understanding of supercritical fluid extraction must begin with an understanding of what occurs in the simplest, binary system case. However even binary systems can have very complicated phase diagrams.

Phase diagrams are generally classified according to the appearance of their pressure-temperature (P-T) projections. The following nomenclature and symbols are used in this discussion:

- Solid, liquid and gas phases are designated by S, L and G respectively.
- Phase boundaries for pure components are shown by solid lines on the P-T projections.

- Critical points for pure components are shown by open circles on the P-T projections.
- The loci of critical points produced by changing compositions are shown by dashed lines on the P-T projections.
- The lines along which three phases can exist in equilibrium are shown as dotted and dashed lines on the P-T projections. These three-phase coexistence lines are designated by the phases which coexist at the lines (for example, LLG or SLG).
- Three-phase coexistence lines may terminate at either upper or lower critical end points, designated UCEP or LCEP, and shown as solid circles on the P-T projections.

The P-T projection of a pure substance generally resembles that shown in Figure 1. Its simplicity is partially a result of the phase rule, which dictates that two-phase equilibrium must be represented by a line on a P-T projection, and that three-phase equilibrium must be represented by a point (ie. the triple point). However, the phase rule also suggests that the P-T projection of a binary system is more complex. Two-phase equilibrium is represented by a surface, while a line represents three-phase equilibrium. Four-phase equilibrium, which is impossible in the case of a pure substance, is shown by a point.

One major type of binary system occurs where the triple point temperature of the heavy component lies well below the critical point temperature of the light component. The high pressure phase behavior of such systems involves only fluids. Scott and van Konynenberg [13] have defined six classes of binary fluid systems, as shown in Figure 3. Classes I to V are predicted by the van der Waals equation of state.

Class VI is observed in some aqueous systems. Variations of these types occur in systems having azeotropes.

The simplest binary fluid systems are class I. In this case the pure component critical points are joined by a critical locus produced by changing compositions. The critical locus represents the upper boundary of a surface on the P-T projection on which liquid and gas exist in equilibrium. Beyond this line, the two components are completely miscible. Class I systems occur in mixtures of similar components such as methane-propane or argon-krypton.

If there is some size and/or polarity difference between the components, a class II system may result. This is similar to a class I system, except that there is a three-phase LLG coexistence line below the vapor pressure curve of the light component. The LLG line terminates at the UCEP. A critical locus for liquid-liquid equilibrium extends upwards from the UCEP. The surface bounded by the LLG line and the liquid-liquid critical locus represents liquid-liquid equilibrium. At the LLG boundary, the liquids are in equilibrium with a gas phase. Below the LLG line gas-liquid equilibrium exists, while beyond the critical locus the liquid phases become miscible. Examples of class II systems include ammonia-toluene and carbon dioxide-octane.

Larger size and/or polarity differences result in class III systems. The LLG line now cuts the gas-liquid critical locus into two branches. One branch joins the UCEP and the critical point of the light component. The other is connected to the critical point of the heavy component and continues into high pressure regions. Carbon dioxide-water and methane-hydrogen sulfide form class III systems.

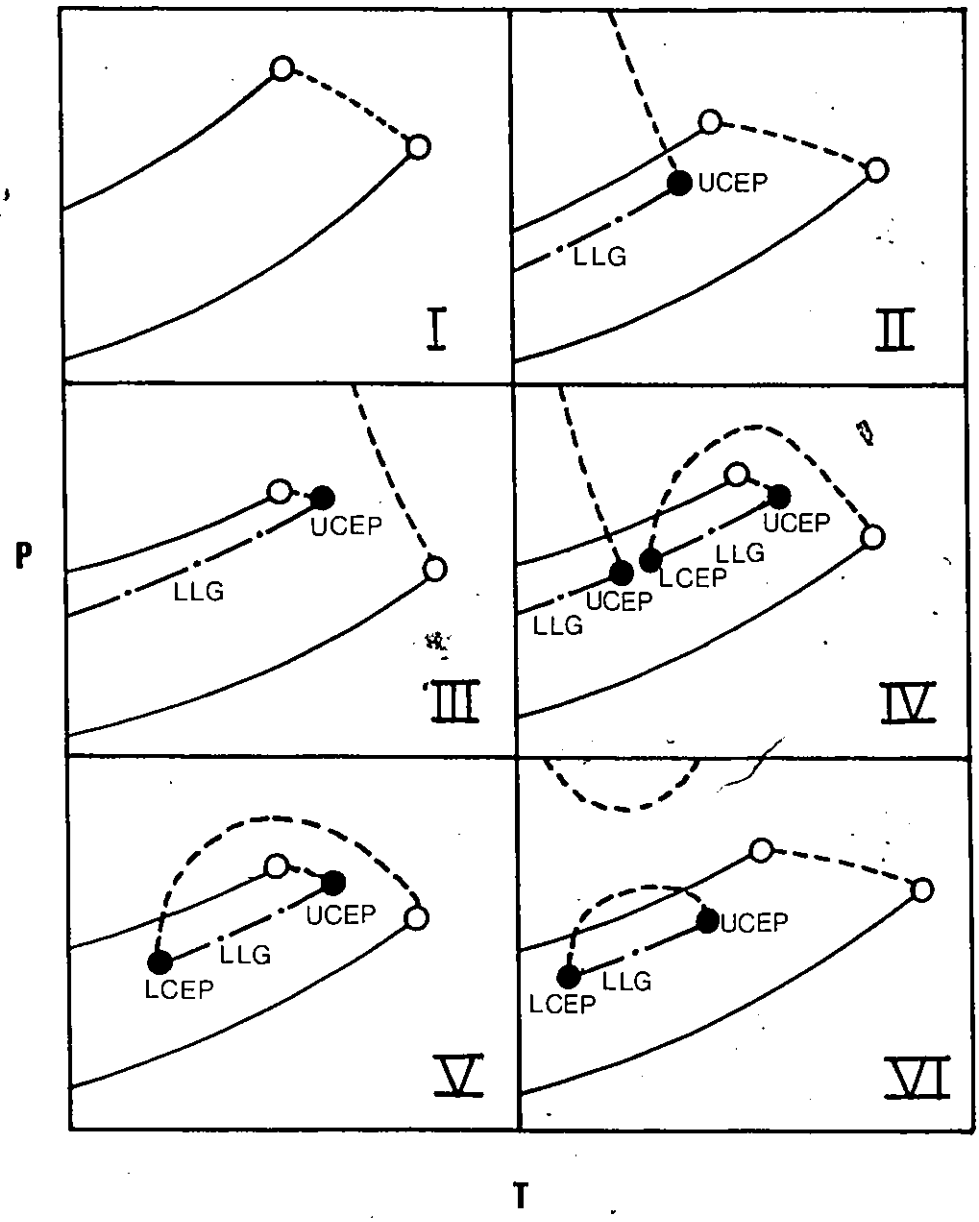

Figure 3: P-T Projections for Binary Fluid Systems.

Substances with large molecular size and/or polarity differences, such as methane-hexane , form class IV systems. These systems are similar to class III, except that the LLG line is cut by the gas-liquid critical locus. This locus now connects a LCEP with the critical point of component 2. A second UCEP connected to a liquid-liquid critical locus is formed at the end of the lower branch of the LLG line. The gap in the LLG line represents a region of liquid phase miscibility.

If the lower branch of the LLG line of a class IV system is absent, a class V system results. There is complete liquid miscibility below the LCEP. An example of a class V system is ethane-ethanol.

Class VI systems are observed only in aqueous mixtures such as deuterium oxide (heavy water)-2-methylpyridine. Class VI systems have a short LLG line, and the UCEP and LCEP are joined by the liquid-liquid critical locus. A second liquid-liquid critical locus exists above the first. In other words, a second region of two immiscible liquid phases exists at high pressures.

A second major type of phase behavior occurs when the triple point temperature of the heavy component is significantly above the critical point temperature of the light component. Such mixtures are often termed asymmetric mixtures. In this case solid-fluid equilibrium may exist. Three types of asymmetric solid-fluid systems are considered here. Figure 4 shows the P-T projections of the three types as classified by Chai [14].

In each case, there is a SLG line with a critical end point (the LCEP) joined to the critical point of the light component by a critical locus. These lines form the boundary of a region of liquid-gas equi-

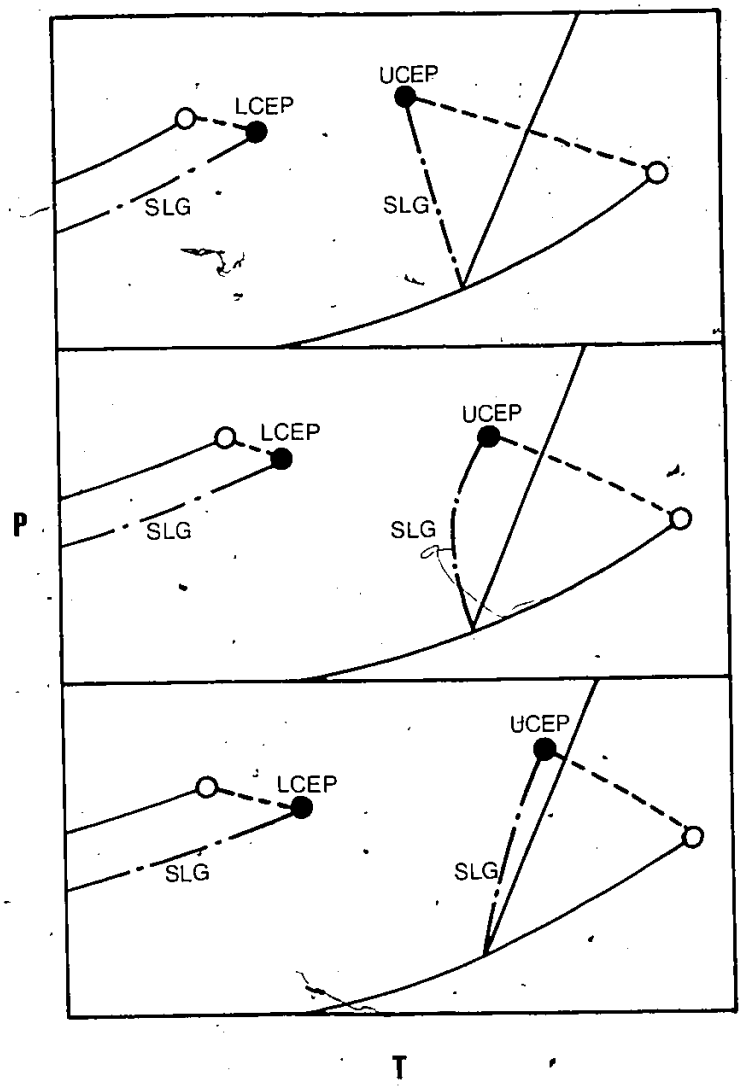

Figure 4: P-T Projections for Binary Solid-Fluid Systems.

librium. The LCEP is usually close to the critical point of the light component, because the mixture in this region is usually dilute in the heavy component. There is another SLG line stretching from the triple point of the heavy component to another critical end point. This is the UCEP, and it is joined to the critical point of the heavy component by a gas-liquid critical locus. The SLG line and the critical locus bound a region of liquid-gas equilibrium. At the SLG line, these two phases are in equilibrium with a solid phase. Beyond the critical locus, the two components are miscible. The shape of the high temperature SLG line is used to distinguish the types of solid-fluid systems.

Systems such as naphthalene-ethylene exhibit behavior similar to that shown in Figure 4(A). The SLG line is negatively sloped. Note that at temperatures between the LCEP and the UCEP no liquid phase can exist. There is only a solid in equilibrium with a supercritical fluid. At temperatures between the UCEP and the solid's triple point, solid-gas equilibrium exists below the SLG line, while liquid-gas equilibrium exists above the SLG line. Here the term gas actually refers to a supercritical fluid.

Naphthalene and carbon dioxide mixtures have a phase diagram similar to that in Figure 4(B). In this case there is a temperature minimum in the SLG line. Therefore the temperatures where only solid-supercritical fluid equilibrium exists range from the LCEP to the minimum in the SLG line. From the temperature of the minimum to the UCEP, liquid-gas equilibrium exists between the branches of the SLG line, while solid-gas equilibrium exists above and below the branches.

A third type of asymmetric binary phase behavior is shown in Figure 4(C). The SLG line is positively sloped. Here exclusive solid-supercritical fluid equilibrium takes place from the LCEP temperature to the triple-point of the heavy component. Between the temperature of the triple point and the UCEP, liquid-gas equilibrium exists below the SLG line, and solid-gas equilibrium exists above. Helium and argon form this type of system.

Other types of binary systems can also occur. These include intermediate types where the temperatures of the critical point of the light component and the triple point of the heavy component are similar, and systems that are extremely asymmetric.

2.2 Solubilities of Solids in Supercritical Fluids

The regions of solid-supercritical fluid equilibrium in asymmetric binary mixtures have received much attention. One reason for this attention is that these mixtures are often representative of systems of interest. For example, many of the solids studied are simple compounds which are homologs of complex aromatic compounds found in coal and heavy oils. Another reason for studying solid-supercritical fluid equilibrium is its simplicity. There can only be one type of phase equilibrium in these systems if the regions described above are studied. In addition, the solubility of the supercritical fluid in the solid can be assumed to be insignificant. Therefore, only the composition of the supercritical phase needs to be measured. Thermodynamic description and modelling of the system is greatly simplified if the solid is assumed pure.

As remarked by Kurnik et al. [15], there exist few published data for the solubility of solids in supercritical fluids. There has been an increase in the gathering of data in recent years, but there is still a need for more. Table 2 summarizes most of the measurements which have been made for the solubilities of solids in supercritical fluids.

By far the most common solvents studied are carbon dioxide and ethylene, and the most common solute studied is naphthalene. The results obtained generally resemble those shown in Figure 2. Solubility increases with increasing pressure at all temperatures, with the largest rate of increase taking place near the critical pressure. At high pressures, the solubility reaches a limiting value which increases with temperature. However, at pressures near the critical pressure, solubility decreases with increasing temperature. The highest solute loadings are observed near the UCEP temperature.

Many methods have been used to obtain solubility data for the systems shown in Table 2. These methods are outlined in Section 3.1.

Table 2: Solid-Supercritical Fluid Solubility Measurements.

Solvent	Solute	Year	Reference
water	quartz	1935	[16]
ethylene	naphthalene	1948	[17]
ethylene	hexachloroethane naphthalene	1950	[18]
ethylene	naphthalene	1953	[19]
ethylene	p-chloroiodobenzene hexachloroethane	1953	[20]
helium hydrogen argon nitrogen methane ethylene	naphthalene	1962	[21]
carbon dioxide	diphenylamine	1962	[22]
ethane	naphthalene	1963	[23]
ethylene carbon dioxide	naphthalene	1964	[2]
ethylene ethane carbon dioxide methane	phenanthrene	1964	[24]
methane ethylene carbon dioxide	naphthalene	1966	[25]
water	quartz	1973	[26]
ethylene	naphthalene phenanthrene anthracene	1979	[27]
carbon dioxide	naphthalene biphenyl	1980	[28]
carbon dioxide	phenol p-chlorophenol 2,4-dichlorophenol	1980	[29]
carbon dioxide	dimethylnaphthalene	1981	[15]
ethylene	phenanthrene benzoic acid hexachloroethane		
ethane ethylene carbon dioxide	naphthalene hexamethylbenzene fluorene triphenylmethane anthracene phenanthrene pyrene	1982	[30]
xenon	naphthalene	1984	[33]
carbon dioxide	naphthalene	1985	[32]

Chapter III

EXPERIMENTAL

This section details the experimental aspects of the research. Experimental techniques employed by other researchers are discussed first. The equipment, materials and methods used in this work are then described.

3.1 Experimental Techniques

Researchers have used several techniques to measure the solubilities of solids in supercritical fluids. There are two major types of techniques: static methods, in which equilibrium is achieved in a closed cell; flow methods, in which equilibrium is achieved by passing the supercritical fluid through a packed bed of solid.

Many researchers have used static methods which involve sampling of the fluid phase. The solid and supercritical fluid are contained in a vessel. When equilibrium is achieved, a small amount of fluid is displaced into a sampling vessel. Pressure fluctuations which might disrupt the equilibrium must be minimized during sampling. A heavy, incompressible fluid such as mercury is therefore often used for the displacement. The composition of the sample is determined by decompressing it and recovering each component. Examples of static sampling techniques occur in the work of Diepen et al. [17] [19] and Eisenbeiss [24].

Other static methods do not involve sampling. Tsekhanskaya et al. [2] place a pellet of solid into a vessel. The vessel is then charged with a measured amount of supercritical fluid. Once equilibrium is achieved, the system is decompressed and the weight lost by the pellet is measured. The solubility is determined from the known amount of solid dissolved in the known amount of supercritical fluid.

A related method involves charging known amounts of supercritical fluid and solid into a variable volume view cell. The isopleth (a line of constant composition) corresponding to the amounts charged is determined by observing the temperatures and pressures at which all of the solid is barely dissolved. Krukonis et al. [31] use this method.

Some researchers use static methods where the composition of the fluid is directly measured. King et al. [21] [25] charge a specially constructed cell with solid and fluid. When equilibrium is achieved, the concentration of solute in the fluid is determined spectrophotometrically. Ewald [20] dopes the solid with a known proportion of radioactive tracer atoms. The composition of the fluid phase can then be determined by measuring its radioactivity.

Some researchers consider static methods to be complex and time consuming. Flow methods are generally simpler. In these, the supercritical fluid flows through the solid. The flowrate is low enough to minimize pressure drop across the bed of solid and to ensure saturation of the fluid phase. The saturated fluid is decompressed across a heated metering valve which also controls the flowrate. Researchers employing flow methods include Johnston [27], van Leer and Paulaitis [29], Kurnik et al. [15], McHugh [33] and Cheong [32]. In most cases, the composi-

tion of the fluid phase is determined by recovering the components as they exit at the metering valve. However, McHugh samples the saturated fluid exiting the bed of solid using a chromatographic sampling valve. The composition of the sample is again determined by decompressing it and recovering the components.

Two methods are used in this work. One is a flow method resembling that used by McHugh, in that a sampling valve is used. The other is a static method in which samples of saturated supercritical fluid are displaced into a sampling valve. Both methods use essentially the same apparatus. The major innovation of this work is that the samples are directly analyzed using a supercritical fluid chromatograph. Solubility measurements are therefore fast and direct. The samples are not decompressed, but remain at supercritical conditions. Therefore problems such as incomplete recovery of solute cannot occur.

3.2 Apparatus

The apparatus consists of two parts: one serves to saturate the supercritical fluid with solute and is termed the saturator; the other part is a modified supercritical fluid chromatograph. The two are linked by a six-way sampling valve, which conveys samples of saturated supercritical fluid from the saturator to the chromatograph. A detailed description of the apparatus follows, using letters and numbers which refer to parts of the apparatus and valves respectively as labelled in Figure 5.

3.2.1 Saturator

Gas supplied from a cylinder (A) is compressed to the desired pressure by a booster pump (B). The pump is a Futurecraft model 90739 automatic pressure intensifier. It consists of two cylinders connected by a differential area piston. Compressed air is supplied through a hand loading pressure regulator to the large diameter cylinder. The resulting piston movement compresses the gas supplied to the small diameter cylinder. When the piston reaches the limit of its stroke, the air in the large cylinder is vented and the cycle is repeated. Outlet pressure is a maximum of 10000 psig (69 MPa) and is controlled by adjusting the pressure in the large cylinder.

Compressed gas from the booster pump passes through a buffer (C) which reduces the magnitude of pressure fluctuations. The buffer is simply a stainless steel cylinder of large internal volume. It has been pressure tested to 35 MPa.

After passing through the buffer, the path of flow is controlled by a series of valves (1,2,3). These are Autoclave Engineers SW series non-regulating valves with 11000 psig (76 MPa) maximum allowable pressure.

Opening the three-way valves (1,3) and closing the two-way valve (2) causes flow to pass through two solute columns (D) in series. Each of these is a stainless steel cylinder of 25 cm length and 1 cm internal diameter, pressure tested to 35 MPa. They are packed with alternating layers of powdered solute and glass wool. Closing the three-way valves and opening the two-way valve causes flow to bypass the solute columns.

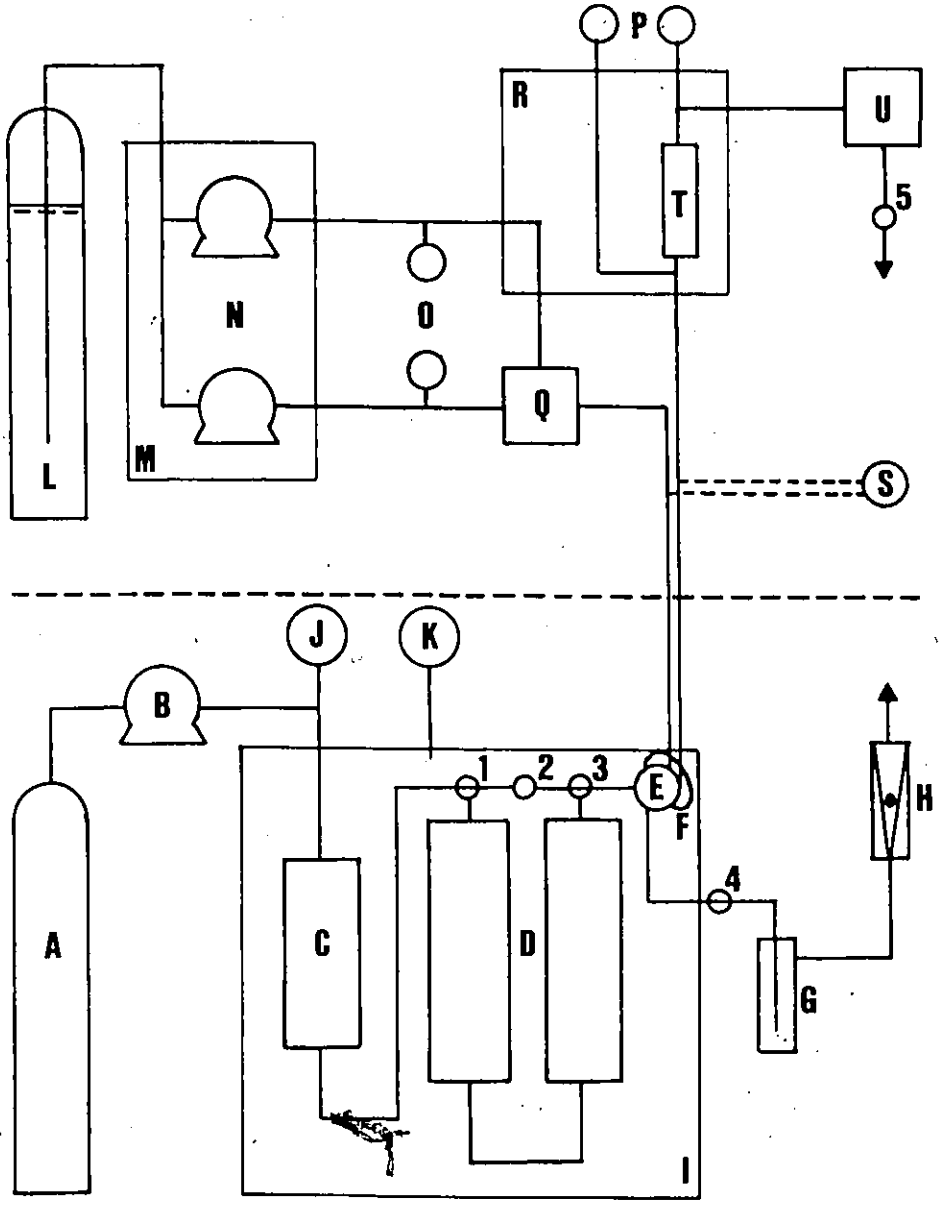

Figure 5: Diagram of the Apparatus. A: cylinder. B: booster pump. C: buffer. D: solute columns. E: sampling valve. F: sample loop. G: cold trap. H: rotameter. I: temperature controlled equipment. J: pressure gauge. K: quartz thermometer. L: cylinder with dip tube. M: refrigerated bath. N: pumps. O: flow transducers. P: pressure gauges. Q: mixing chamber R: column oven. S: injection valve. T: column. U: detector. 1-5: valves.

The flow from valve 3 passes through the six-way sampling valve (E). This is a Valco C6U six-port injector, with a maximum allowable pressure of 5000 psig (35 MPa). In the "load" position, flow passes through a Valco SL100 0.1 mL sample loop (F). In the "inject" position, the sample loop is connected to flow from the chromatograph. To ensure smooth and consistent switching of the valve, a Valco AH60 helical drive air actuator is used.

The flow from the sampling valve is vented through the outlet valve (4). One of two valves is used here, depending on the sampling method used (see below). If the displacement method is used, then the outlet valve is an Autoclave Engineers SW series two-way non-regulating valve with 11000 psig (77 MPa) maximum allowable pressure. If the flow method is used then the outlet valve is a Whitey 31RF2 two-way micrometering valve with 5000 psig (35 MPa) maximum allowable pressure. It is wrapped in electric heating tape and kept at a temperature above the melting point of the solute in order to avoid fouling by solid. Outlet flowrate is monitored using a Matheson 602 rotameter (H). A cold trap (G) between the outlet valve and the rotameter prevents the accumulation of solute in the rotameter.

The tubing used in the saturator is stainless steel. It has 1/8 in. (3.175 mm) outer diameter, except for 1/16 in. (1.5875 mm) tubing connected to the sampling valve, and 1/4 in. (6.35 mm) tubing joining the solute columns. All fittings are stainless steel, and are either Swagelok, Autoclave Engineers Speedbite or Valco ZVN (sampling valve fittings only).

The temperature of the apparatus within the box (I) on Figure 5 is controlled. The buffer and solute columns are contained in a recirculating water bath. The temperature is thermostatically controlled within ± 0.05 K. The valves, the sampling valve and the sample loop are wrapped with electric heating tape. The temperature is manually controlled within ± 0.2 K.

Pressure is measured by a U.S. Gauge Company 0 to 5000 psig (34 MPa) Bourdon tube gauge (J), with 10 psi (68.95 kPa) increments, and readable to the nearest 5 psi (35 kPa). Temperature is measured to the nearest 0.01 K by a Hewlett-Packard 2801A quartz thermometer with a 2850D probe (K). The thermometer is calibrated to the IPTS-68 scale using a triple point water bath and a platinum resistance thermometer.

3.2.2 Supercritical Fluid Chromatograph

The composition of sample from the six-way valve is analyzed using a supercritical fluid chromatograph. This is a Hewlett-Packard 1082B high-performance liquid chromatograph modified to use supercritical carbon dioxide as mobile phase. The only significant differences from a standard liquid chromatograph are the use of a cooling bath to increase pumping efficiency for liquid carbon dioxide, and the use of a back pressure regulator to control system pressure. Other mobile phases can be used if they are compatible with the operation of the chromatograph.

The chromatograph is supplied with liquid mobile phase from a cylinder equipped with a dip tube (L). The mobile phase is filtered by a 2 micron frit and is cooled to below 263 K by a Nesslab RTE-Z4 refrigerated recirculating bath (M). Liquid from the bath is also used to cool the two chromatograph pumps (N) below 263 K, at which temperature liquid carbon dioxide can be pumped with high efficiency.

The chromatograph pumps are of the reciprocating diaphragm type. They operate at constant volumetric flowrate. The flowrate is measured by means of flow transducers (O). The pressure developed by the pumps is controlled by a back-pressure regulator (5) at the outlet of the flow system of the chromatograph. The maximum allowable pressure is 40.0 MPa. The pressure is measured by Bourdon tube gauges (P) at the inlet and outlet of the column.

After leaving the pumps, the fluid streams pass through pulse dampers and are mixed in a chamber (Q). Prior to mixing, one of the streams is preheated in the column oven (R).

One of two injectors can be used to introduce sample into the supercritical fluid chromatograph. The injector supplied with the chromatograph is a manually operated Rheodyne 7125 syringe-loading six-way valve (S). In the "load" position the sample loop on the injector can be partially or completely filled by liquid sample using a syringe. In the "inject" position, the sample loop is connected to the flow from the chromatograph. The other injector is the Valco six-way valve (E) described previously. The valve is connected to the flow of mobile phase by approximately 0.8 m of 1/16 in. (1.5875 mm) diameter stainless steel tubing, heated to the column oven temperature by electric heating tape.

Injected samples are conveyed by the supercritical fluid mobile phase to the chromatographic column (T) in the column oven. At this point the mobile phase is a supercritical fluid. The column is 100 mm in length and 4.6 mm in diameter, and contains particles of Hypersil 5 micron ODS as a stationary phase.

The separated components eluting from the column pass through a variable-wavelength ultraviolet-absorbance detector (U). This consists of a high-pressure cell having windows through which light from a deuterium lamp can shine. The intensity of light of a particular wavelength exiting the cell is compared with the intensity of light at a reference wavelength. These intensities are measured by photodiodes which scan the ultraviolet-absorbance spectrum obtained from a diffraction grating. The signal from the detector is integrated using a built in integrator.

Except for pressure control, the operation of the chromatograph is controlled by a remote terminal. The flowrate of mobile phase can be varied from 0 to 10.00 mL/min. in 0.01 mL/min. increments. The oven temperature may be set from 5 K above ambient temperature to 373 K in 1 K steps. The detector wavelength varies from 190 to 600 nm in 1 nm steps. The reference wavelength must have at least a 60 nm difference from the detector wavelength. The main variable affecting the integrator is slope sensitivity, which can be varied from 0 to 81.00 in steps of 0.01.

Measurements on the chromatograph are made by starting a "run" from the remote terminal. The detector signal is recorded on a plotter. Peaks produced by substances passing through the detector are integrated and the peak areas are reported. The times between the start of the run and the detection of the peaks (the retention times) are also recorded.

3.3 Materials

The solids used in this work are naphthalene, anthracene and biphenyl. Naphthalene and biphenyl are obtained from Fisher Scientific. These chemicals exceed 99 % purity. Anthracene is obtained from Aldrich Chemical Company and has a purity exceeding 99.9 %.

The fluids used as solvents in this work are carbon dioxide and ethylene. The carbon dioxide is obtained from Air Products, while the ethylene is obtained from Matheson. The minimum purity of these fluids is 99.9 %.

The fluids used as mobile phases in the chromatograph are carbon dioxide and nitrous oxide. They are obtained in liquid form in cylinders equipped with dip tubes. They have a minimum purity of 99.9 %.

Acetone is used as a liquid solvent. It is obtained from Canlab, and has a purity exceeding 99.9 %.

Several properties of the materials used throughout this work are summarized in Table 3. The critical pressure and acentric factor for anthracene are not available. They are estimated using the Gunn-Yamada method and the Lee-Kesler method respectively, as presented in Reid et al. [34]. The values obtained agree with those calculated by Johnston [27].

In addition to the properties given in Table 3, the compressibility factors of pure carbon dioxide and ethylene, are needed. These are obtained from high precision equations of state developed by IUPAC [36] [37]. Appendix A summarizes the equations and gives computer programs used to calculate the compressibility factors.

Table 3: Properties of the Materials Used in this Study.

The vapor pressures of the solids are given by the Antoine equation log(P) = A-B/(T-C) where P is vapor pressure in Pa and T is temperature in K. The coefficients for naphthalene and anthracene are from Johnston et al. [30], while those for biphenyl are from Boublik et al. [35].

Material	Molecular weight	Critical properties		Acentric factor
		Temperature K	Pressure MPa	
Carbon dioxide	44.01	304.2	7.376	0.225
Ethylene	28.05	282.4	5.036	0.085
Naphthalene	128.17	748.4	4.053	0.302
Biphenyl	154.21	789	3.85	0.364
Anthracene	178.23	883	3.30	0.455

Solid	Molar volume	Antoine coefficients		
	mL/gmol	A	B	C
Naphthalene	128.6	13.575	3729.3	0
Biphenyl	155.5	9.37031	1998.725	70.417
Anthracene	142.6	12.147	4397.6	0

3.4 Methods

As mentioned above, two methods of solubility measurement are used. One is a static method with displacement sampling, while the other is a flow method. Each method is described below, again making use of letters and numbers which refer to parts of the apparatus and valves respectively as labelled on Figure 5.

The solids are pulverized in a mortar and pestle before use. Alternating layers of pulverized solid and glass wool are packed into the solute columns (D). Each column contains approximately 60 % by volume of solid.

Once the apparatus is assembled, it is thoroughly purged of air by the fluid being used. All valves are then closed. The desired temperature is set on both the bath and heating tape (I). The desired pressure for the pump (B) is set. The operating conditions of the chromatograph are selected. The same conditions are used for all solubility measurements. These are detailed in Appendix B.

In the displacement method, the solute columns (D) are at first charged with supercritical fluid at high pressure (20 to 25 MPa) through valve 1. The valve is closed, and approximately 2 hours are allowed for the system to reach equilibrium. Samples of saturated supercritical fluid are taken by opening valves 1 and 3 in sequence while the sampling valve (E) is in the "sample" position. Pure fluid entering through valve 1 displaces saturated fluid through valve 3. Valves 1 and 3 are then closed, and the sampling valve is switched to the "inject" position. A chromatograph run is simultaneously started. Sample peak areas are measured on the chromatograph, and the sampling valve (E) is

returned to the "load" position. The sample line is vented through valve 4. It is then cleared of any residual solute by pure solvent admitted through valve 2. Finally the line is vented and all valves are closed. The system is now ready for another sample. The pressure of the system can be lowered by repeating the sampling procedure without opening valve 1. The pump (B) is adjusted to the new pressure. Samples can be taken immediately, since the fluid will still be saturated (because solubility decreases with pressure at constant temperature).

In the flow method, valves 1 and 3 are open. The micrometering valve (4) is adjusted so that a steady flowrate of less than 200 mL/min. of gas at ambient conditions is obtained. The flowrate is checked by a previously calibrated rotameter (H). Cheong [32], using similar equipment, found that this flowrate ensured saturation. The sampling valve (E) is kept in the "load" position. Samples of the saturated supercritical fluid leaving the solute columns (D) are taken by switching the valve to the "inject" position. A chromatograph run is simultaneously started, and peak areas are measured. The sampling valve is returned to the "load" position. New samples can be taken immediately. The sampling line is periodically cleared of any accumulation of solid by closing valves 1 and 3 and opening valve 4, thus allowing pure supercritical fluid to flow through.

Chapter IV

RESULTS AND DISCUSSION

The main objective of this research is to establish a method of determining solubilities in supercritical fluids through the use of supercritical fluid chromatography. This section develops such a method from the experimental results. A calibration equation is derived, and a calibration factor is determined for the naphthalene-carbon dioxide system. It is shown how the method can be easily extended to other solutes and fluids without remeasuring the calibration factor. The results are correlated using an equation of state.

4.1 Measuring Peak Areas

In this section, the displacement and flow methods of sampling are compared and the consistency of peak areas is evaluated. The naphthalene-carbon dioxide system is used for these evaluations.

The measurements for carbon dioxide saturated with naphthalene at 308.2 K are shown in Appendix B. Both the flow method and the displacement method are used. It is apparent that the peak area of naphthalene varies somewhat from sample to sample. The averages of the results and their 95 % confidence intervals are given in Figure 6.

Both the displacement and the flow method appear to give essentially the same peak areas. However, the flow method gives considerably more precise peak areas than the displacement method. The confidence inter-

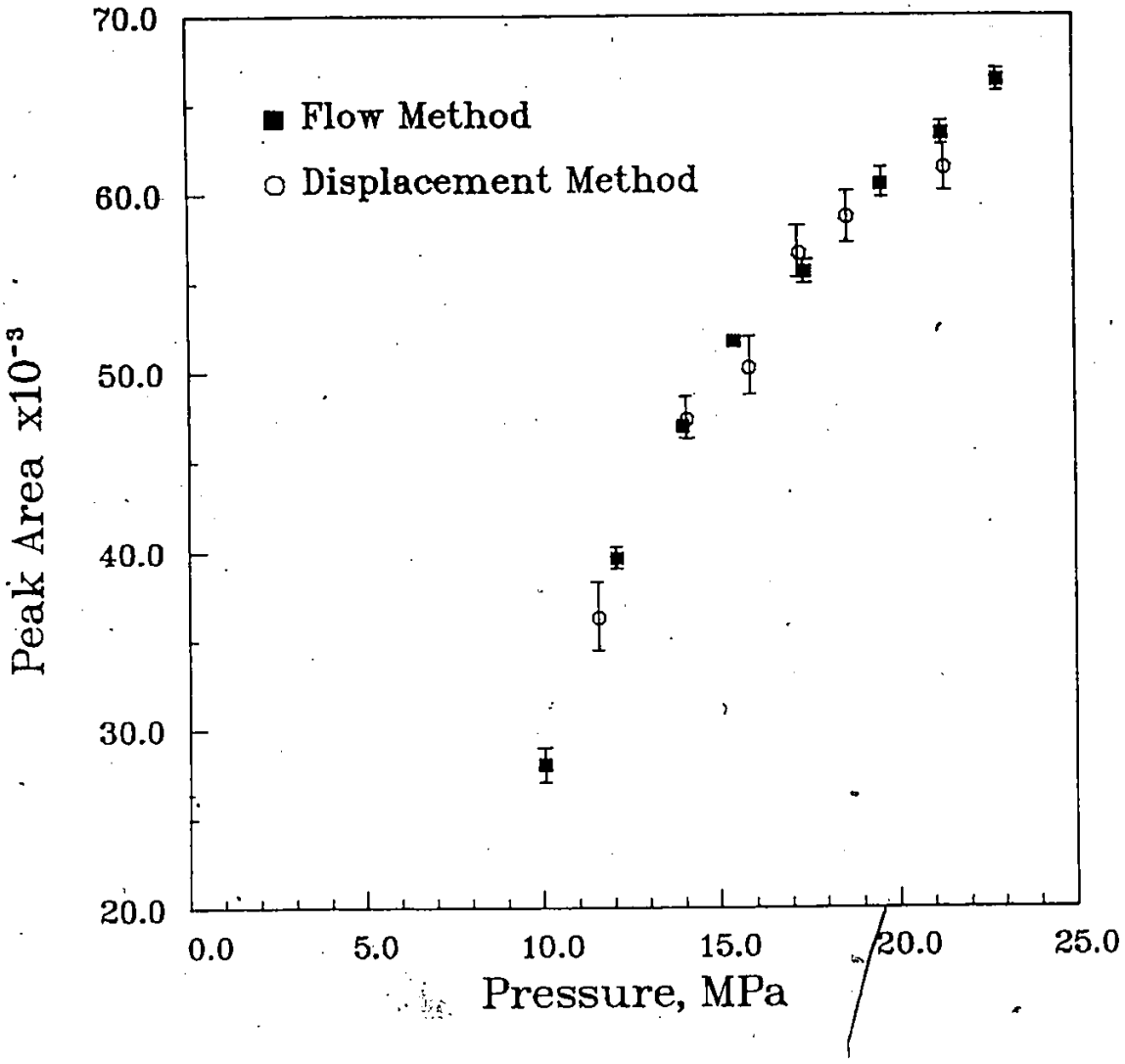

Figure 6: Comparison of the Flow and Displacement Methods. Average peak areas and 95 % confidence intervals for the naphthalene-carbon dioxide system at 308.2 K.

vals are generally 1 to 3 % of the peak size in the case of the flow method, while they range from 2 to 5 % of the peak size in the displacement method.

There are several sources of uncertainty in the peak areas. Fluctuations in the chromatograph operating conditions occur. The mobile phase flowrate is observed to vary by as much as ± 1.5 %. Another source of uncertainty is fluctuation in the saturator temperature and pressure. Temperature fluctuations are small (± 0.2 K) and probably insignificant. Pressure fluctuations are slight in the flow method (± 0.1 MPa), however sampling during the displacement method is observed to be accompanied by a momentary pressure drop of as much as 0.5 MPa. This accounts for the lower precision of the displacement method.

4.2 Calibration Method

Several methods are used to measure compositions by chromatography. Most of these involve comparing the peak areas of individual components and the use of a calibration factor. For example, if two components 1 and 2 in a sample produce peak areas of s_1 and s_2 respectively, then

$$(n_1/n_2) = c_{12}(s_1/s_2) \qquad (1)$$

where n_1 and n_2 are the number of moles of components 1 and 2 respectively. The value of the constant c_{12} is a function of detector wavelength. Other chromatographic variables have negligible effect on c_{12}, since they tend to affect all peak areas in equal proportion. It should be noted that this relationship applies only if the peak area is proportional to the total quantity of a component. This is the case for

the supercritical fluid chromatograph, which uses an ultraviolet-absorbance detector obeying the Beer-Lambert law.

Most supercritical fluid chromatographs use ultraviolet-absorption detectors. There is a problem in applying equation 1 when an ultraviolet detector is used. Most of the solvents of interest in supercritical fluid extraction have low ultraviolet absorbances [38]. These solvents may therefore produce no peak on the chromatograph.

Tests are done to check if the solvents used in this work can produce peaks on the detector. Samples of pure solvent are injected from the saturator, and peak areas are measured over the entire detector wavelength range (190 to 600 nm in 10 nm steps). No carbon dioxide peaks can be observed when nitrous oxide is used as the mobile phase in the chromatograph. Small and inconsistent ethylene peaks are observed when carbon dioxide is used as a mobile phase.

These results indicate that equation 1 cannot be applied to the measurement of solubilities in this work. Another expression, based on solute peak size and the properties of pure solvent, is derived below.

The mole fraction of solute (2) in supercritical fluid (1) can be expressed as

$$y_2 = n_2/(n_1 + n_2) \qquad (2)$$

The number of moles of solute n_2 is proportional to the peak area from the chromatograph, thus

$$n_2 = f_2 s_2 \qquad (3)$$

where f_2 is a constant characteristic of the solute. The value of f_2 is a function of the operating conditions of the chromatograph, namely column inlet pressure, column oven temperature, mobile phase flowrate and detector wavelength.

If the mixture is sufficiently dilute, then it will have properties close to those of the pure supercritical fluid. The number of moles of mixture can then be approximated by

$$n_1 + n_2 = PV/(Z_1RT) \tag{4}$$

where P, V and T are the pressure, temperature and volume of the mixture, Z_1 is the compressibility factor of pure supercritical fluid at the pressure and temperature of the sample, and R is the gas constant. Note that the volume of the mixture is equal to the volume of the sample loop and is therefore constant.

Substituting equations 3 and 4 into equation 2 gives

$$y_2 = c_2 s_2 Z_1 T/P \tag{5}$$

where

$$c_2 = f_2 R/V \tag{6}$$

The calibration factor c_2 is a function of chromatograph pressure, oven temperature, mobile phase flowrate, detector wavelength and sample loop volume. If these are held constant, then c_2 will be constant.

Equation 5 can be used to calculate solubility from experimental data. The validity of the equation rests with the assumption that the

properties of a dilute supercritical mixture can be approximated by the pure supercritical fluid. To test this assumption, the molar volume of pure carbon dioxide is compared to that of carbon dioxide saturated with naphthalene. Figure 7 clearly shows that differences in molar volume are small.

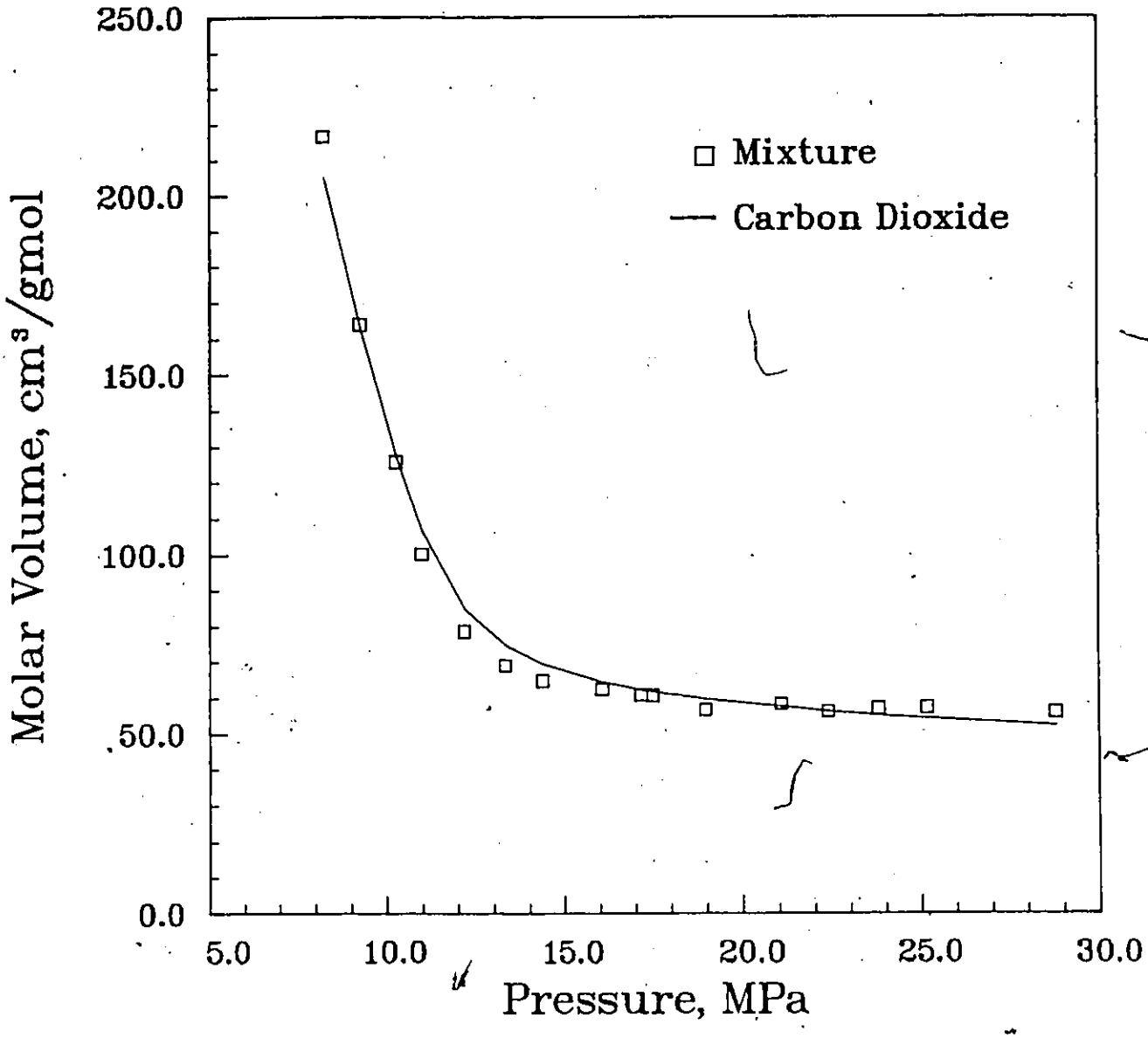

Figure 7: Molar Volume of Carbon Dioxide Saturated with Naphthalene. Comparison of the molar volume of carbon dioxide saturated with naphthalene at 328.2 K [33] with that of pure carbon dioxide [36].

4.3 Determination of the Calibration Factor

The calibration factor c_2 can be obtained for naphthalene by comparing the peak areas reported in Appendix B to the solubility results of other workers. Cheong [32] has obtained solubility results for the 308.2 K isotherm of the carbon dioxide-naphthalene system which agree well with those of other wofkers [22] [33]. He used a flow method with apparatus very similar to that in the saturator in this work. His results are therefore used for the determination of the calibration factor.

Average peak areas obtained using the flow method are shown in Table 4. Values of mole fraction interpolated from Cheong's data are also shown. Values of the compressibility factor of pure carbon dioxide are obtained from the IUPAC equation of state given in Appendix A.

The best value of c_2 is found using the method of least squares. The expected mole fraction, designated y_2^*, is obtained from Cheong's data. The calculated mole fraction is obtained from equation 5. Thus the quantity to be minimized is

$$\Sigma \, (y_2^* - c_2 s_2 Z_1 T/P) \qquad (7)$$

where the summation is over all the points given on Table 4. The best value of c_2 is found to be 0.04641. Note that this value applies only to chromatographic operating conditions as given in Appendix B.

Table 4: Data for Calibration Factor Determination.

The system is naphthalene-carbon dioxide at 308.2 K, measured using the flow method. This table gives the data required for Equation 7.

Pressure P MPa	Peak Area s_2	Expected y_2	Compressibility Z_1
10.07	27957	0.0101	0.24151
12.10	39605	0.0128	0.27000
13.96	46970	0.0144	0.29927
15.41	51572	0.0154	0.32256
17.41	55605	0.0163	0.35482
19.58	60523	0.0171	0.38981
21.30	63323	0.0177	0.41762
22.89	66295	0.0181	0.44284

4.4 Experimental Results

In this section the solubility measurements are presented and are compared to those of other workers. The actual measurements are given in Appendix B. The average peak areas and their 95 % confidence intervals are reported here. Each result represents the average of four to six measurements. Compressibility factors calculated from the IUPAC equations shown in Appendix A are also given here. Mole fractions calculated from Equation 5 are given with 95 % confidence intervals. These intervals assume that all of the uncertainty derives from peak area measurement, and that the uncertainties from other sources are insignificant.

4.4.1 Naphthalene-Carbon Dioxide

The calibration factor for naphthalene has been obtained above. In order to test the method of solubility measurement, results for the naphthalene-carbon dioxide system are presented and are compared to those obtained by other workers.

The results for the 308.2 K isotherm are shown in Table 5 and are compared to those of other workers in Figure 8. All points are within a 95 % confidence interval of the results of McHugh [33] and Cheong [32]. There is some deviation from the results of Tsekhanskaya et al. [22] at high pressures.

The good agreement with previous workers noted above is not surprising, since the calibration factor is obtained by fitting results to previous data for the 308.2 K isotherm. A better test of the calibration test is to compare results for another isotherm. The results for the 318.2 K isotherm are given in Table 6 and are compared to those of

Tsekhanskaya et al. [2] in Figure 9. Again there is good agreement, with all points except one being within a 95 % confidence interval of previous results.

The naphthalene-carbon dioxide system has a phase diagram similar to that shown in Figure 4(B) [33]. The LCEP temperature is 307.7 K [2], and the temperature of the minimum in the SLG line is 331.0 K [33]. The results therefore represent solid-supercritical fluid equilibrium.

Table 5: Solubility of Naphthalene in Carbon Dioxide at 308.2 K.

The calibration factor is 0.04641.

Pressure MPa	Peak area	Compressibility	Mole fraction
Flow method			
10.07	27975 ± 875	0.24151	0.00960 ± 0.00030
12.10	39605 584	0.27000	0.01264 0.00019
13.96	46970 59	0.29927	0.01440 0.00002
15.41	51724 363	0.32256	0.01549 0.00011
17.41	55605 510	0.35482	0.01621 0.00015
19.58	60523 845	0.38981	0.01723 0.00024
21.30	63323 624	0.41762	0.01776 0.00018
22.89	66295 698	0.44284	0.01835 0.00019
Displacement method			
11.58	36253 ± 1755	0.26221	0.01174 ± 0.00057
14.07	47364 977	0.30089	0.01449 0.00030
15.82	50224 1542	0.32927	0.01495 0.00046
17.27	56636 1507	0.35269	0.01654 0.00044
18.62	58648 1376	0.37430	0.01686 0.00040
21.37	61400 1277	0.41859	0.01720 0.00036

Table 6: Solubility of Naphthalene in Carbon Dioxide at 318.2 K.

The calibration factor is 0.04641. The flow method is used.

Pressure MPa	Peak area	Compressibility	Mole fraction
10.27	15898 ± 1422	0.26804	0.00613 ± 0.00055
12.13	31386 671	0.30375	0.01161 0.00025
13.34	51228 552	0.30026	0.01703 0.00018
14.82	58430 798	0.32203	0.01875 0.00026
17.03	68560 546	0.36486	0.02169 0.00017
19.51	79590 735	0.40185	0.02421 0.00022
21.96	88520 1002	0.43882	0.02612 0.00030

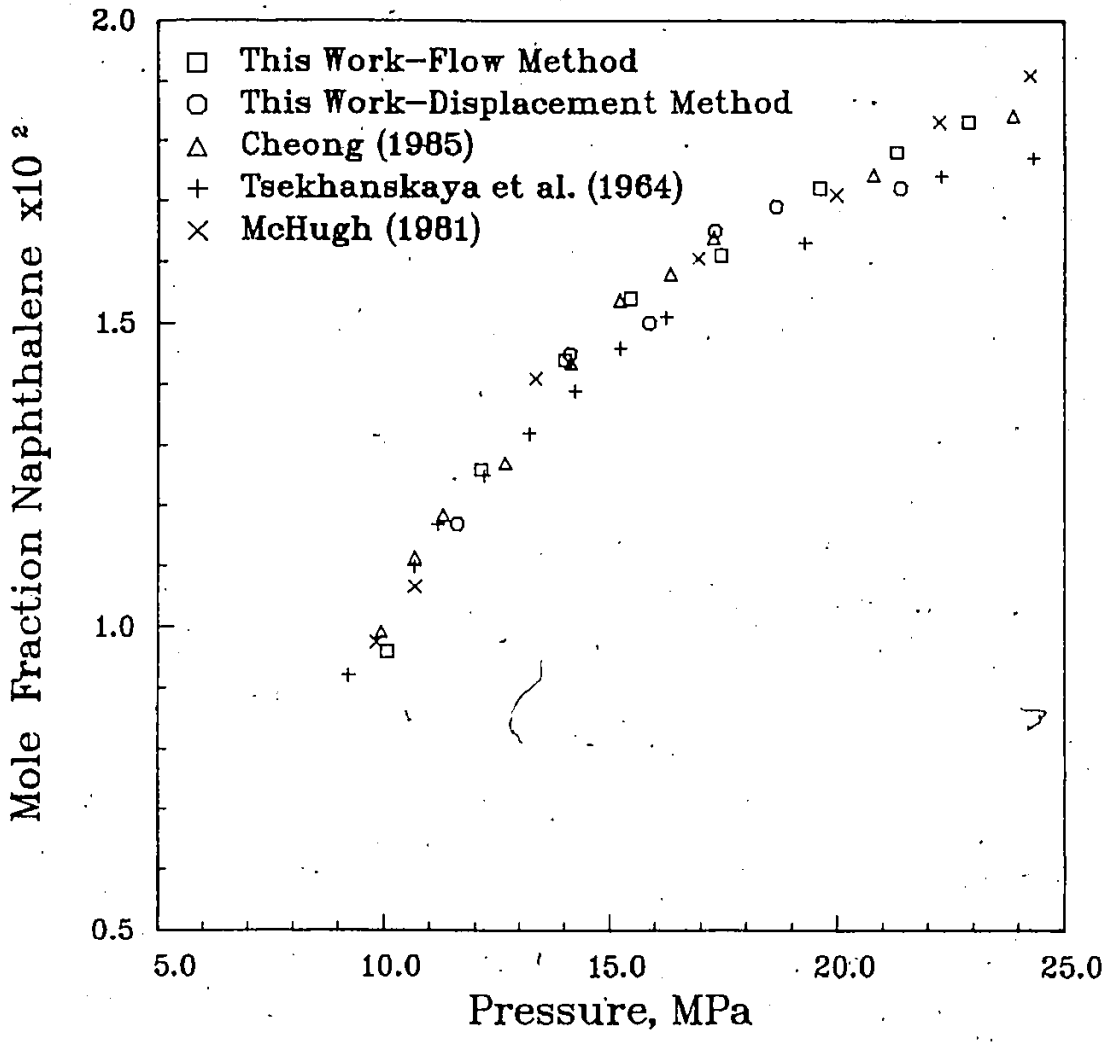

Figure 8: Solubility of Naphthalene in Carbon Dioxide at 308.2 K.

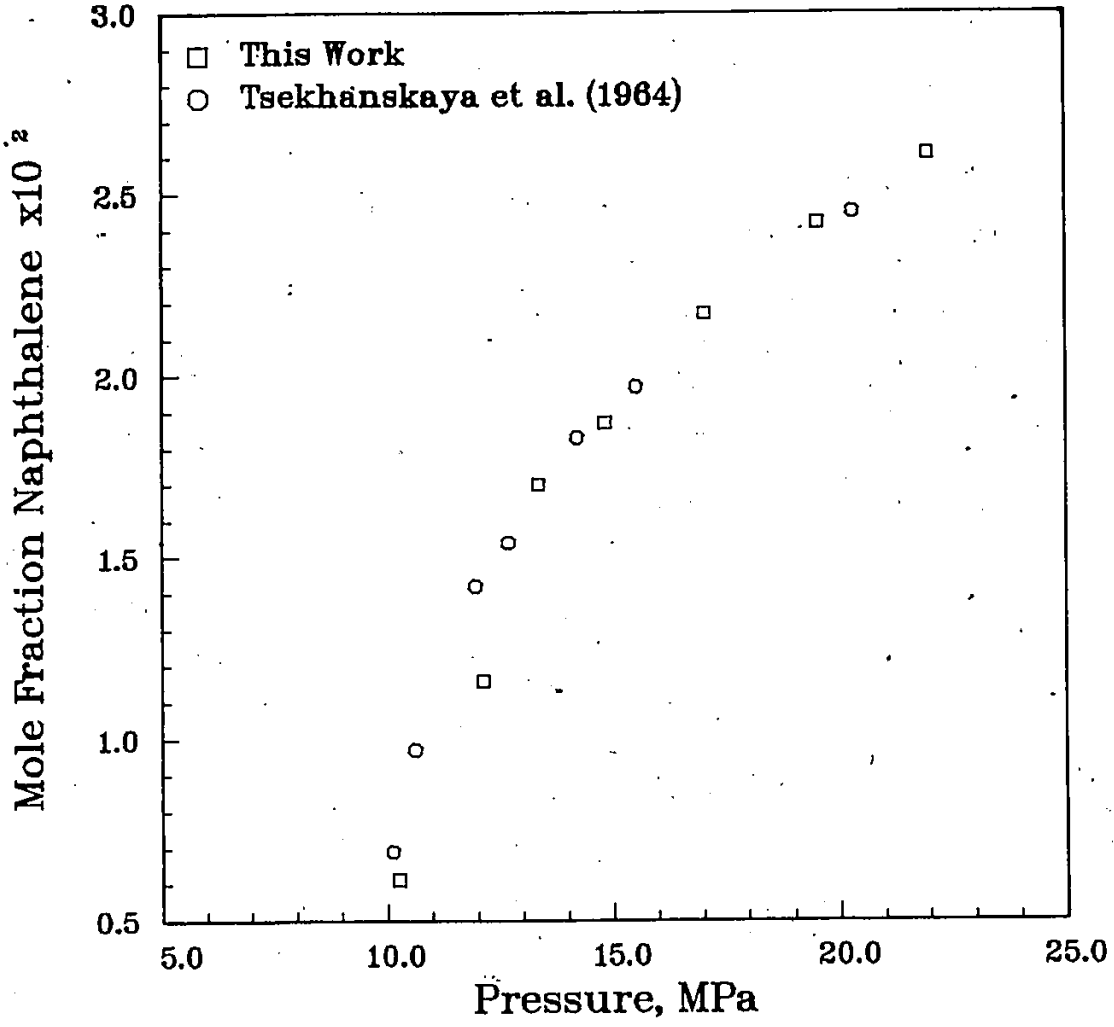

Figure 9: Solubility of Naphthalene in Carbon Dioxide at 318.2 K.

4.4.2 Anthracene-Carbon Dioxide

In order to obtain solubility measurements for a new system, the calibration factor of the solute must be known. The calibration factor for other solutes can be readily obtained from that for naphthalene, as explained below.

Equation 3 relates the number of moles of a component and its peak area on the chromatograph. For two components, the ratio of the number of moles of each component is related to the ratio of their peak areas by Equation 1. If the peak areas for both components are measured using the same chromatographic operating conditions, the equations can be combined to yield

$$c_{12} = f_1/f_2 \qquad (8)$$

The calibration factor c_i is related to the constant f_i by equation 6. If the same sample loop volume is used in sampling mixtures of both components, equations 6 and 8 can be combined to give

$$c_{12} = c_1/c_2 \qquad (9)$$

Note that the value of c_{12} depends only on the detector wavelength, and is independent of the actual chromatographic operating conditions. The calibration factors c_1 and c_2 must apply to identical chromatographic operating conditions and sample loop sizes. However, c_{12} can take different detector wavelengths into account.

In this study, the value of c_{12} is determined by direct injection of samples of known composition into the chromatograph. Details of this procedure and the actual results are given in Appendix C. The value of

c_{12} for anthracene (1) and naphthalene (2) is 0.001182 + 0.000014. The calibration factor for anthracene as calculated from Equation 9 is 4.185×10^{-5}.

The results for the 308.2 K and 323.2 K isotherms of the anthracene-carbon dioxide system are shown in Table 7 and are compared to those of Johnston et al. [30] in Figure 10. The results of this work are within a 95 % confidence interval of those of Johnston et al. for the 323.2 K isotherm. Note that the less precise displacement method is used in this case. This is because the flow method could not be used, since the outlet valve could not be heated to the melting point of anthracene.

The phase behaviour of the anthracene-carbon dioxide system has not been studied. However, since the mole fraction of anthracene is very low, the LCEP is probably close to the critical temperature of carbon dioxide, namely 304.2 K. The SLG line probably exists at temperatures close to the melting point of anthracene, namely 489.5 K. Therefore the results obtained above probably represent solid-fluid equilibrium.

Table 7: Solubility of Anthracene in Carbon Dioxide.

The calibration factor is 0.00005486. The displacement method is used.

Pressure MPa	Peak area	Compressibility	Mole fraction x 10000
Temperature = 308.2 K			
11.03	77523 ± 3091	0.25430	0.302 ± 0.012
12.10	98450 4447	0.27012	0.372 0.017
14.20	127967 2927	0.30314	0.462 0.011
16.34	150150 2529	0.33762	0.525 0.009
18.62	177200 3920	0.37446	0.603 0.013
21.17	191480 5589	0.41544	0.635 0.019
Temperature = 323.2 K			
11.96	37540 ± 3995	0.33562	0.186 ± 0.020
13.82	100510 3259	0.33907	0.437 0.014
15.93	174880 4876	0.36162	0.704 0.020
17.79	245125 8325	0.38622	0.944 0.032
19.65	284525 6115	0.41233	1.009 0.022
21.79	319375 9107	0.44332	1.152 0.033
23.86	352175 8141	0.47368	1.240 0.029

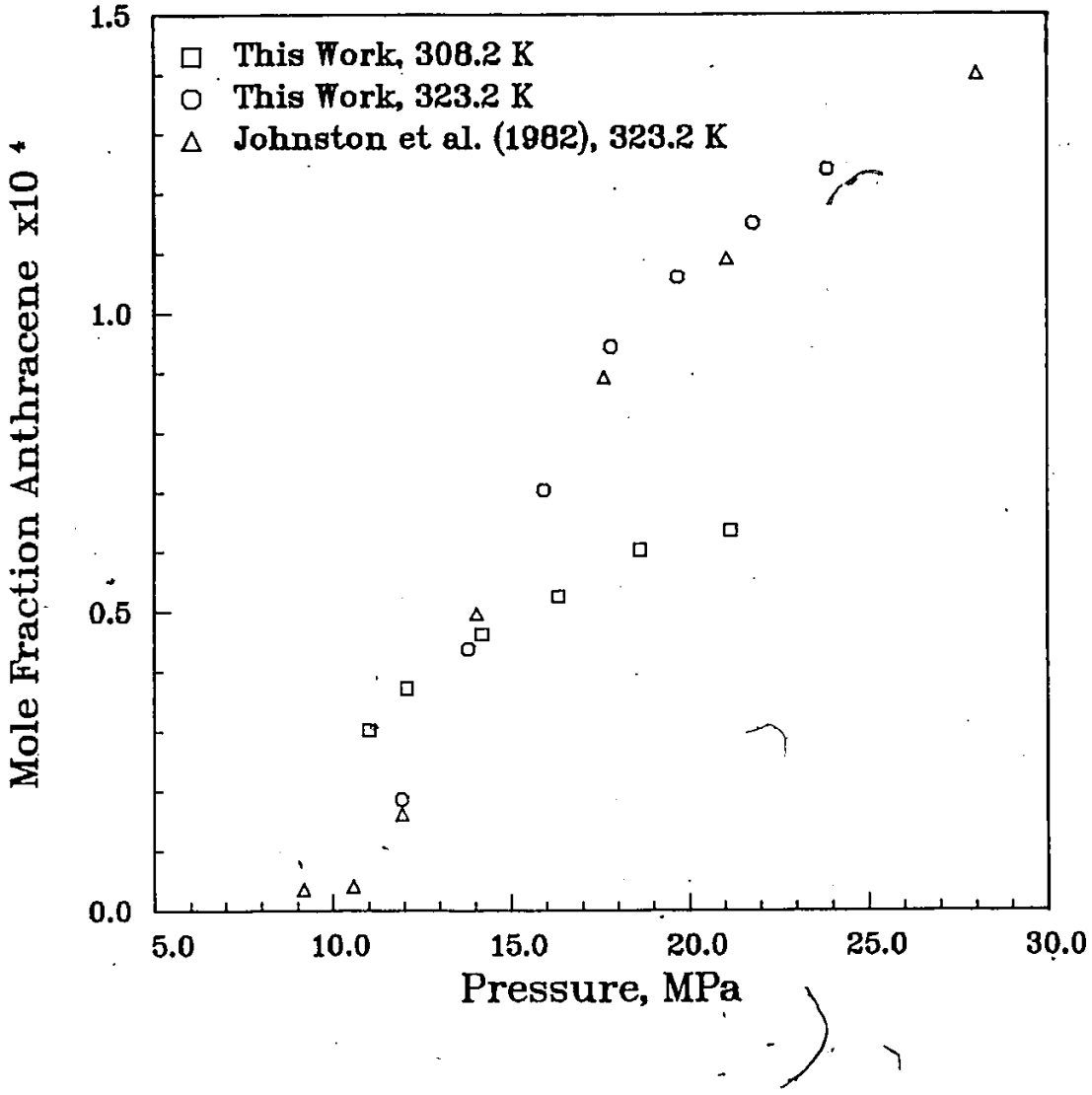

Figure 10: Solubility of Anthracene in Carbon Dioxide.

4.4.3 Biphenyl-Carbon Dioxide

The calibration factor for biphenyl can be determined by the same procedure used above for anthracene. The c_{12} for biphenyl-naphthalene cannot be directly obtained, since their peaks are not completely separated on the chromatograph. Instead the c_{12} for biphenyl (1) and anthracene (2) is determined. From Appendix C, the value of c_{12} is 1109 + 1.5. The value of the calibration factor for biphenyl obtained from Equation 9 is therefore 0.006084.

The results for biphenyl at 308.2 K are shown in Table 8 and are compared to the results of McHugh [33] for the 309.0 K isotherm in Figure 11. The results compare well with those of McHugh.

The biphenyl-carbon dioxide system has a phase diagram similar to that shown in Figure 4(B) [33]. The LCEP is at 305.2 K [39], and the minimum in the SLG line is at 321.7 K [33]. The results therefore represent solid-supercritical fluid equilibrium.

Table 8: Solubility of Biphenyl in Carbon Dioxide at 308.2 K.

The calibration factor is 0.006084. The flow method is used.

Pressure MPa	Peak area	Compressibility	Mole fraction
10.31	238950 ± 3508	0.24445	0.01062 ± 0.00016
13.10	270975 3858	0.28560	0.01108 0.00016
14.55	288850 4258	0.30869	0.01149 0.00017
16.06	323800 6278	0.33304	0.01259 0.00024
18.51	354160 3839	0.37367	0.01341 0.00015
20.58	391180 4696	0.40593	0.01447 0.00017
22.10	398475 5877	0.43170	0.01460 0.00022
24.41	420400 3948	0.46695	0.01508 0.00014

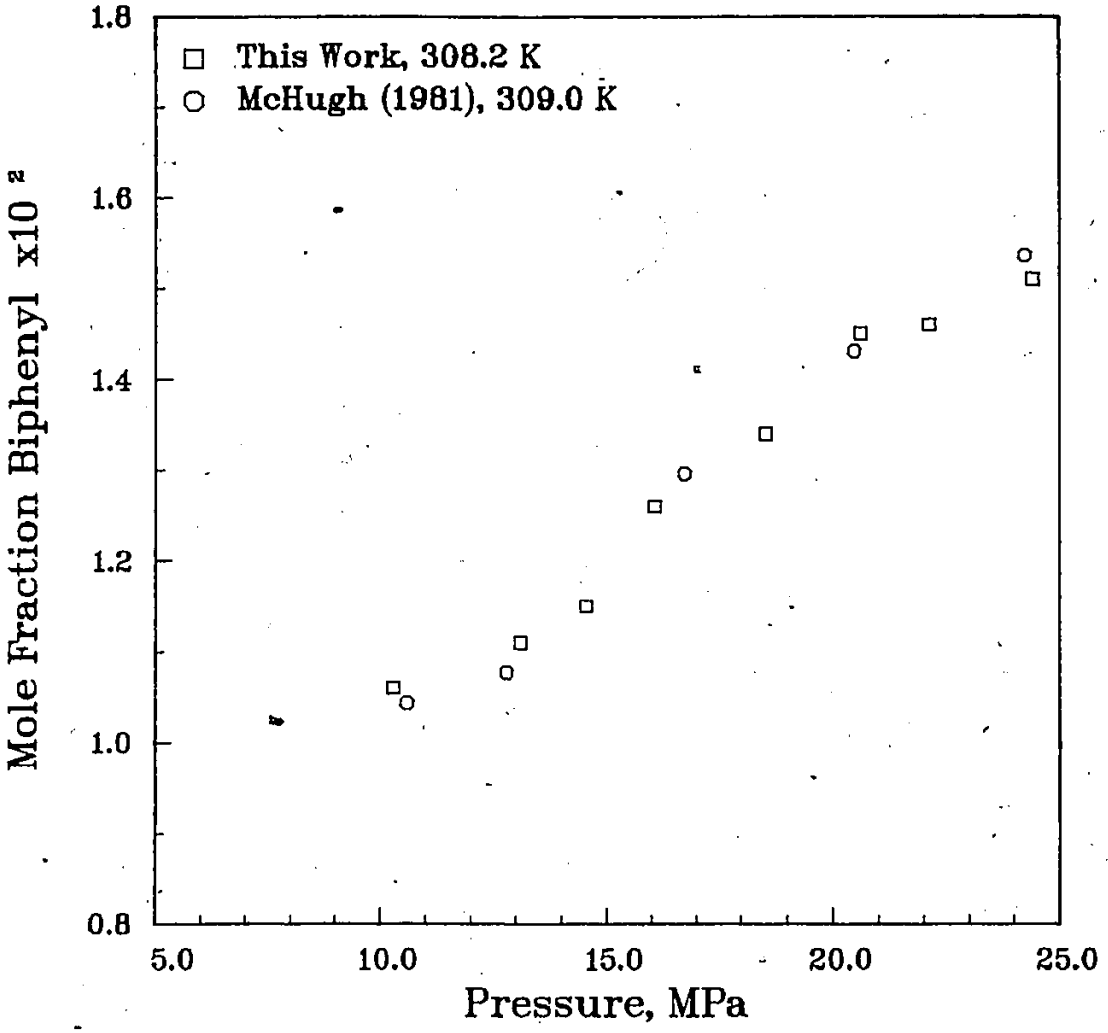

Figure 11: Solubility of Biphenyl in Carbon Dioxide.

4.4.4 Anthracene-Ethylene

In Equation 5, the effect of the actual solvent used is reflected in the compressibility factor. The solvent should have no effect on the calibration factor. In order to show this, ethylene is used as a solvent instead of carbon dioxide.

The results for the anthracene-ethylene system at 308.2 K and 323.2 K are shown in Table 9 and are compared to those of Johnston [27] in Figure 12. The results are within a 95 % confidence interval of those of Johnston for the 323.2 K isotherm. Again the less precise displacement method is used, for the same reason stated for the anthracene-carbon dioxide system.

The phase behaviour of this system has not been studied. However, for the same reasons discussed for the anthracene-carbon dioxide system, these results probably represent solid-supercritical fluid equilibrium.

Table 9: Solubility of Anthracene in Ethylene.

The calibration factor is 0.00005486. The displacement method is used.

Pressure MPa	Peak area	Compressibility	Mole fraction x 10000
Temperature=308.2 K			
11.31	43744 ± 2952	0.39565	0.259 ± 0.014
12.89	68800 4615	0.42317	0.382 0.017
14.93	99184 4128	0.46374	0.521 0.012
16.58	122767 3685	0.49814	0.624 0.010
18.10	143000 4942	0.53032	0.708 0.014
20.72	171080 4406	0.58616	0.818 0.020
Temperature=323.2 K			
13.38	62200 ± 3475	0.47376	0.390 ± 0.022
15.62	150050 6507	0.50673	0.864 0.037
17.79	205183 4758	0.54523	1.115 0.026
19.55	241560 3733	0.57845	1.267 0.020
21.41	298180 5903	0.61448	1.517 0.030
22.82	343940 8335	0.64211	1.716 0.042

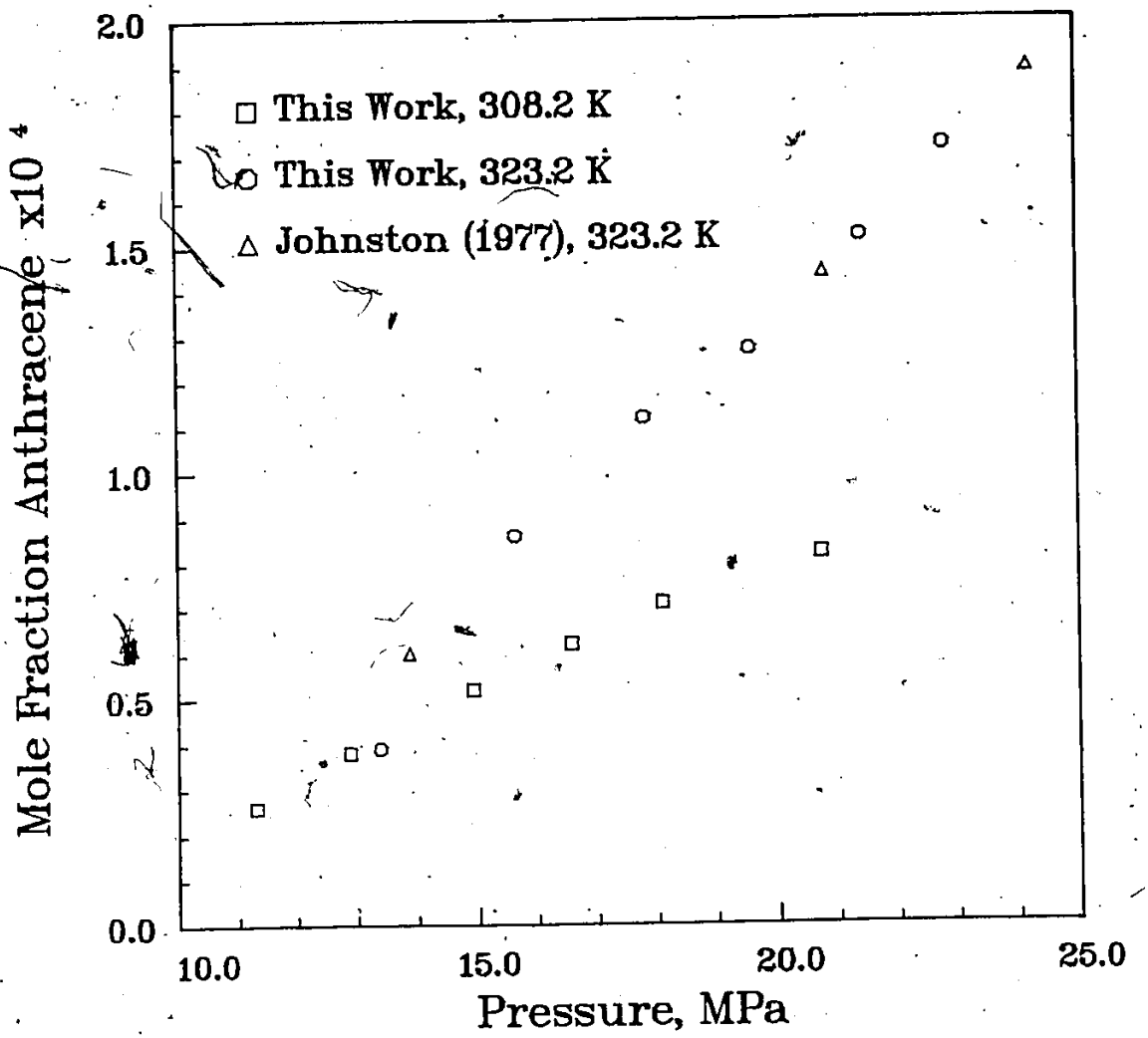

Figure 12: Solubility of Anthracene in Ethylene.

4.5 Correlation of the Results

The correlation of solid-supercritical fluid solubility data is relatively straightforward. This is because the assumption of pure, incompressible solid phase leads to a simple thermodynamic expression. The data obtained in this work are correlated using an equation of state approach.

If a binary solid-supercritical fluid system is in equilibrium, then both phases must have equal temperature T and pressure P, and chemical potentials of both components must be equal in both phases. From the definition of fugacity it follows that at equilibrium, for the solid (component 2)

$$f_2^S = f_2^F \tag{10}$$

where f_2 designates the fugacity, and the superscripts S and F refer to the solid and fluid phases respectively.

The fugacity of a component in the fluid phase can be obtained from the definition of the fugacity coefficient,

$$f_2^F = y_2 \phi_2^F P \tag{11}$$

where ϕ_2^F and y_2 are the fugacity coefficient and mole fraction respectively of component 2 in the fluid phase. The fugacity coefficient can be calculated from a pressure explicit equation of state using the well-known expression

$$RT\ell n(\phi_2^F) = \int_V^\infty [(\partial P/\partial n_2)_{T,V,n_1} + RT/V]dP - RT\ell n(Z) \tag{12}$$

where V and Z are the volume and compressibility factor of the fluid, and n_i is the number of moles of component i.

An expression for the fugacity of the solid is now derived. If the solid is pure, then by definition

$$d\mu_2^S = RT\, d\ell n(f_2^S) \tag{13}$$

where μ_2^S is the chemical potential of the solid. Also, the Gibb's fundamental relation for a pure solid is

$$d\mu_2^S = dG_2^S = -S_2^S dT + v_2^S dP \tag{14}$$

where G_2^S, S_2^S and v_2^S are the molar Gibb's free energy, entropy and volume of the solid component 2 respectively. Combining Equations 13 and 14 at constant temperature gives

$$d\ell n(f_2^S) = v_2^S dP/(RT) \tag{15}$$

Integrating this equation with the assumption of constant molar volume of the solid gives

$$f_2^S = f_2^o \exp[v_2^o(P-P^o)/(RT)] \tag{16}$$

where the superscript o designates a reference state. Let the reference state be saturated solid. Since the saturation pressure for a solid is usually very low, its vapor can be treated as an ideal gas and its fugacity is thus equal to its vapor pressure. Equation 16 therefore becomes

$$f_2^S = P_2^{SAT} \exp[v_2^S(P-P_2^{SAT})/(RT)] \tag{17}$$

where P_2^{SAT} is the vapor pressure of the solid.

Equating the fugacity expressions of Equations 11 and 17 gives the final expression

$$y_2 = (P_2^{SAT}/P)(1/\phi_2^S)\exp[v_2^S(P-P_2^{SAT})/(RT)] \qquad (18)$$

The fugacity coefficient in the fluid phase is obtained from an equation of state through Equation 12, as explained above. In this study, Soave's modification of the Redlich-Kwong equation of state [40]. This equation is

$$P = RT/(v-b) - a(T)/[v(v+b)] \qquad (19)$$

The constants a(T) and b for a pure component are given by

$$a(T) = 0.42747\ [(RT_c)^2/P_c]\ [1+m(1-T_r^{\frac{1}{2}})]^2$$

$$b = 0.08664\ RT_c/P_c$$

$$m \doteq 0.480 + 1.574\,\omega - 0.176\,\omega^2$$

where T_c and P_c are the critical temperature and pressure respectively, ω is the acentric factor and T_r is the reduced temperature. The values of the constants a and b in a mixture are obtained from the pure component constants using the one parameter random mixing rules,

$$a = \Sigma\ \Sigma\ y_i\ y_j\ a_{ij} \qquad (20)$$

$$b = \Sigma\ y_i\ b_i \qquad (21)$$

where

$$a_{ij} = [a_i\ a_j]^{\frac{1}{2}}(1-k_{ij})$$

The parameter k_{ij} represents interactions between the components. It is often found to be a function of temperature. Substituting the Equations 19, 20 and 21 into Equation 12 gives

$$\ln(\phi_2^F) = (b_2/b)(Z-1) - \ln(Z-B) + (A/B)[2(y_1a_1+y_2a_{12})/a-b_2/b]\ln(1+B/Z) \quad (22)$$

where

$$A = a(T)P/(RT)^2$$

$$B = bP/(RT)$$

Equation 18 is fitted to the data in this work. Each isotherm of each system studied is fitted separately. The following objective function is used

$$\Sigma\ (y_2^* - y_2)/y_2^* \quad (23)$$

where y_2^* is the value of y_2 calculated from Equation 18. The objective function is minimized by adjusting the value of k_{ij}.

The experimental data, along with the fitted equations and the fitted values of the parameter are shown in Figure 13, Figure 14, Figure 15 and Figure 16. The fit for the naphthalene-carbon dioxide system (Figure 13) is good at low pressures, but deviates somewhat at higher pressures. The fit for both anthracene-carbon dioxide (Figure 14) and anthracene-ethylene (Figure 16) is good at all pressures. However, the fit for biphenyl-carbon dioxide (Figure 15) is clearly inadequate. One reason for this is that the Antoine equation coefficients used for

biphenyl do not apply to the temperatures studied [35]. Another reason is that the molecular structure of biphenyl is fundamentally different from that of naphthalene or anthracene. Naphthalene and anthracene consist of fused benzene rings, whereas the benzene rings in biphenyl are not fused. This indicates that while the correlation works fairly well for fused ring compounds, it may not be generally applicable to other classes of compounds.

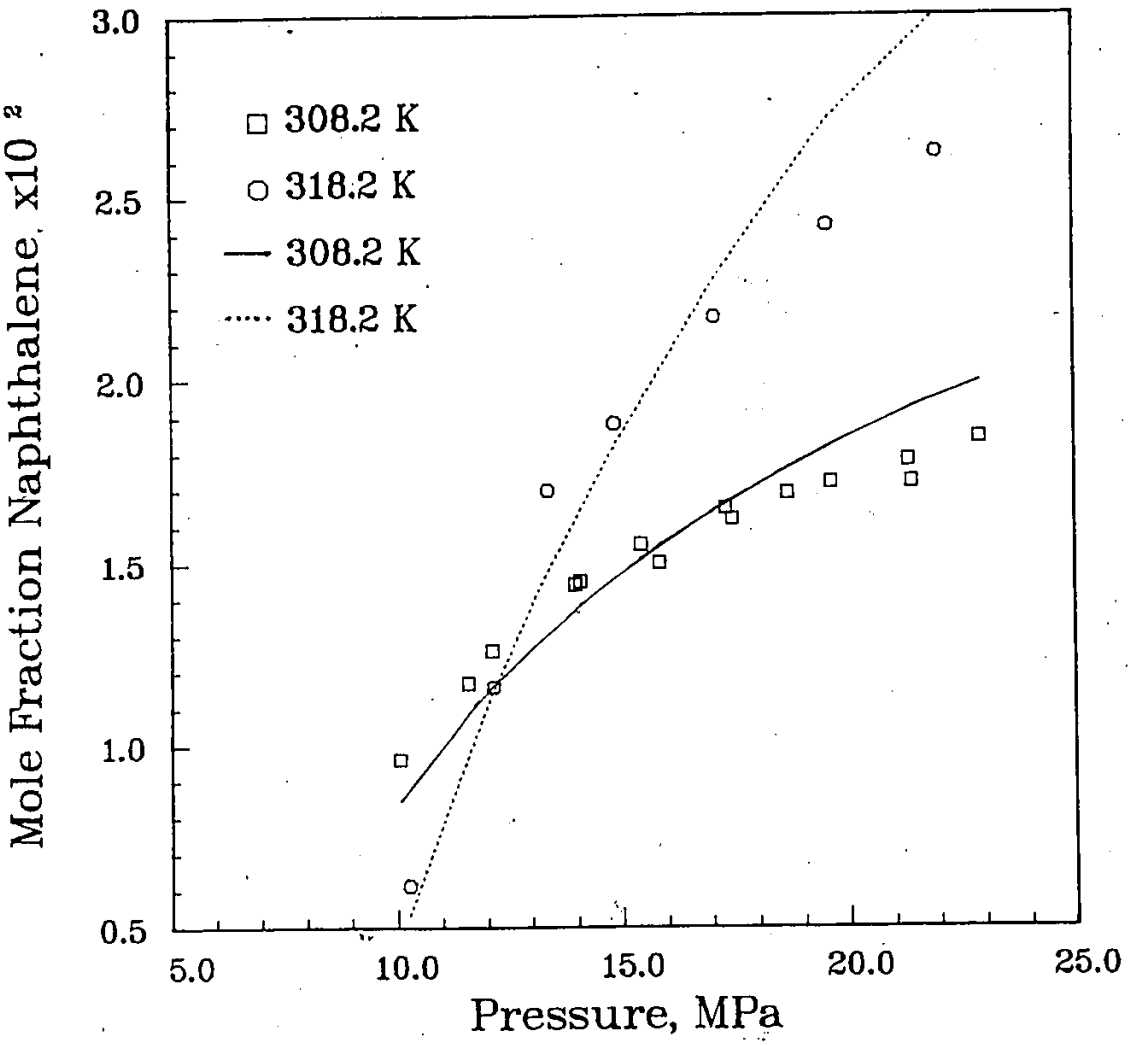

Figure 13: Fitted Equation for the Naphthalene-Carbon Dioxide Data. The value of k_{ij} is 0.10775 at 308.2 K and 0.10629 at 318.2 K.

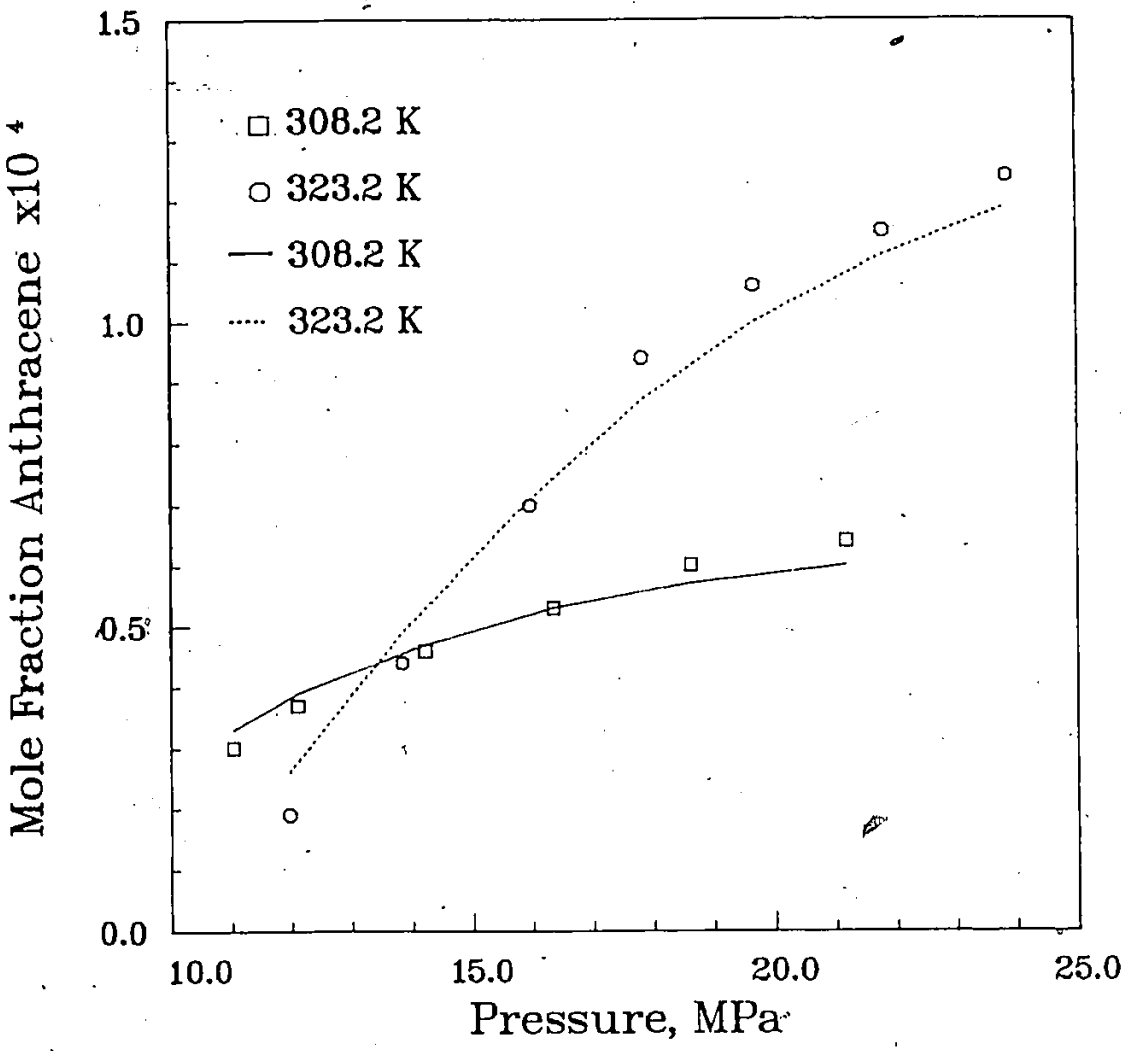

Figure 14: Fitted Equation for the Anthracene-Carbon Dioxide Data. The value of k_{ij} is 0.15916 at 308.2 K and 0.14226 at 323.2 K.

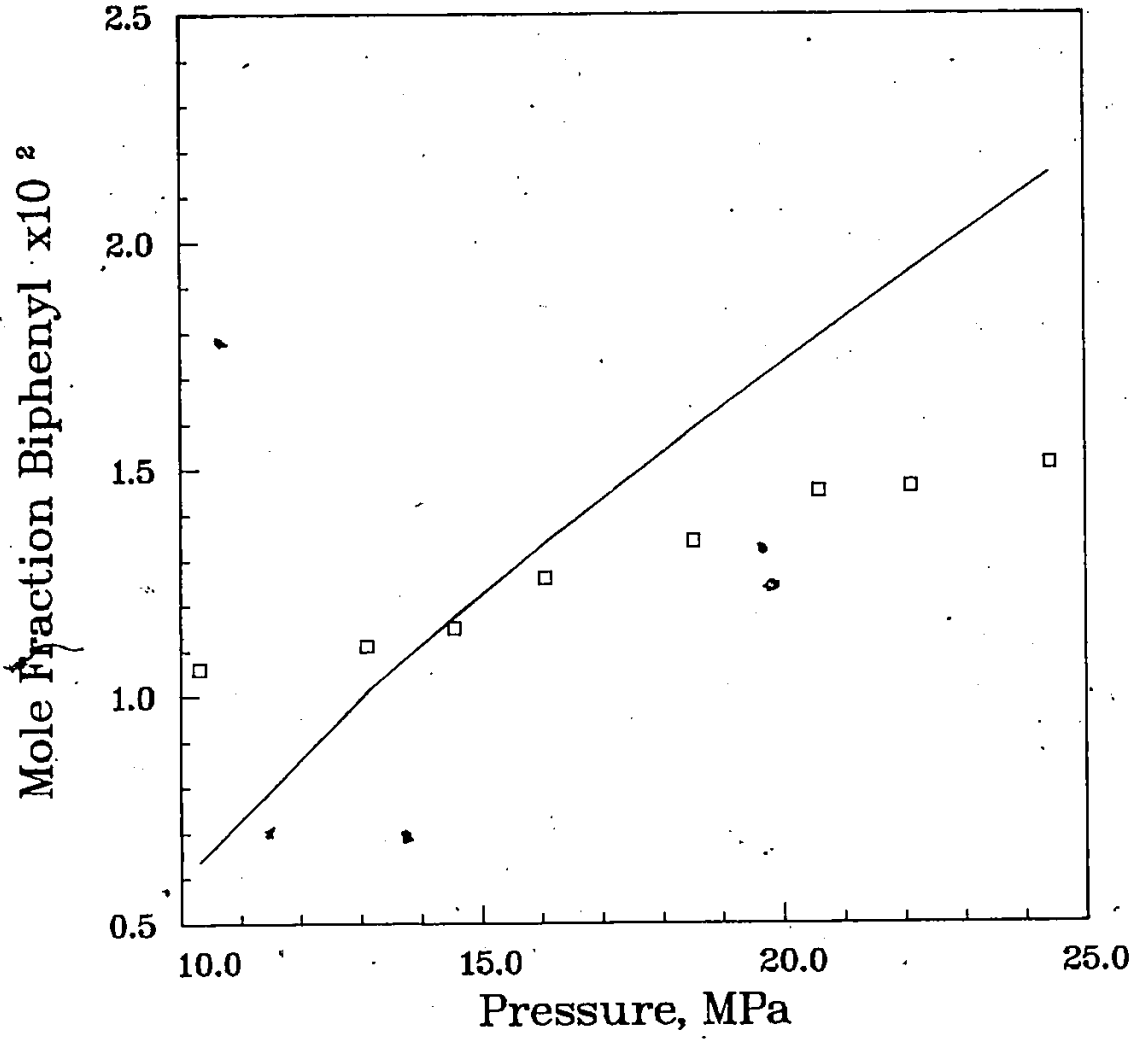

Figure 15: Fitted Equation for the Biphenyl-Carbon Dioxide Data. The value of k_{ij} is 0.13112 at 308.2 K.

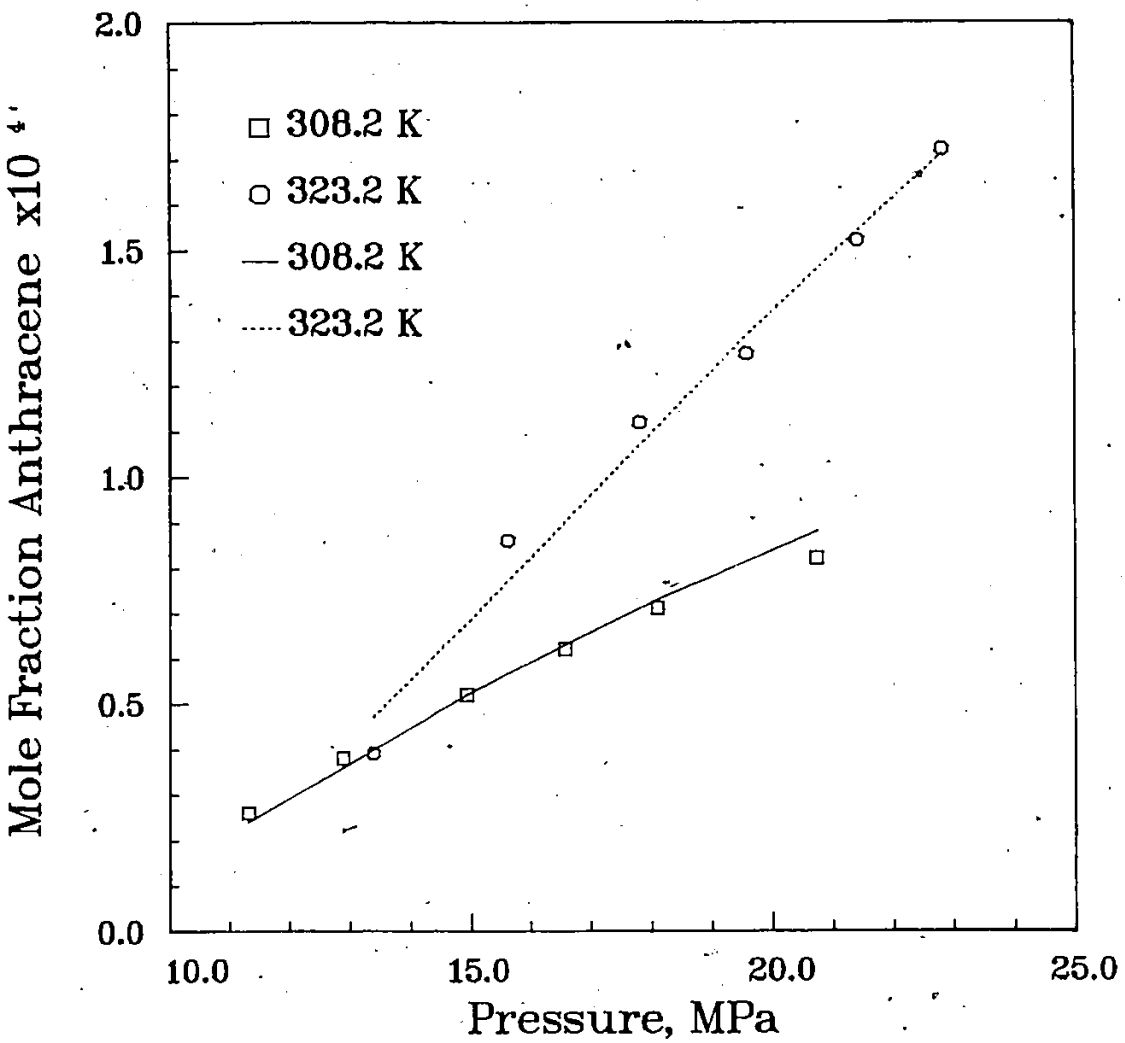

Figure 16: Fitted Equation for the Anthracene-Ethylene Data. The value of k_{ij} is 0.08609 at 308.2 K and 0.06577 at 323.2 K.

Chapter V

CONCLUSIONS

In this research, supercritical fluid chromatography has been applied to the measurement of solubilities of solids in supercritical fluids. Equilibrium between the solid and fluid phases is achieved using either a flow method or a static displacement method. Samples of the saturated fluid phase are directly sampled and analyzed using a supercritical fluid chromatograph.

The flow method is found to give more precise results than the displacement method. This is because a large momentary pressure drop occurs during sampling in the displacement method.

Conventional calibration techniques for the chromatograph cannot be applied. This is because it uses an ultraviolet-absorbance detector which is transparent to most solvents commonly studied in supercritical systems. Tests confirm that this is the case with the solvents used in this work. Therefore a new calibration equation is developed which relates the mole fraction of solute to the compressibility factor of pure solvent and the peak area of solute as measured by the chromatograph.

A calibration factor for naphthalene is determined by comparing measurements for the naphthalene-carbon dioxide system at 308.2 K with results of other researchers. Solubility results for this system at 308.2 K and 318.2 K compare well with previous work.

A simple method is developed which allows calibration factors for other solutes to be determined from that for naphthalene. Calibration factors for anthracene and biphenyl are determined and are used to obtain solubility results for the anthracene-carbon dioxide system at 308.2 and 323.2 K, the biphenyl-carbon dioxide system at 308.2 K and the anthracene-ethylene system at 308.2 and 323.2 K. The results compare well with previous work. The calibration factor is shown to be independent of the solute used.

The results are correlated using the Soave modification of the Redlich-Kwong equation of state. One-parameter random mixing rules are used. Except for the biphenyl-carbon dioxide system, the results are well correlated.

As stated in the introduction, this research is undertaken to develop an improved method of measurement of solubilities in supercritical fluids. This has been largely accomplished. The use of a supercritical fluid chromatograph allows simple and direct composition measurement. The accuracy is at least as good as in existing methods. Calibration factors for new solutes can be easily determined from those already known. Compositions in multiple solute systems can be measured once the calibration factors for individual solutes are known. The simplicity and speed of composition measurement suggests that supercritical fluid chromatography would be useful for on-line analysis in industrial supercritical fluid extraction processes.

Appendix A

EQUATIONS OF STATE FOR CARBON DIOXIDE AND ETHYLENE

High precision equations of state have been developed for carbon dioxide and ethylene by IUPAC [36] [37]. This appendix gives these equations as well as computer programs for their use.

The equation for carbon dioxide is

$$Z = 1 + \Sigma \Sigma b_{ij}(1/T_r - 1)^j(\rho_r - 1)^i \qquad (A.1)$$

where ρ_r is the reduced density and T_r is the reduced temperature. The critical density and temperature are 0.01063 mol/cm and 304.2 K respectively. The values of the coefficients b_{ij} are given in the computer program listing.

The equation for ethylene is

$$Z = \Sigma \Sigma B_{ij}T^{j-1}\rho^{i-1} \qquad (A.2)$$

with ρ in mol/cm^3 and T in K. The values of the coefficients B_{ij} are given in the computer program listing.

```
100 REM ************************************************************************
110 REM * THIS PROGRAM CALCULATES THE COMPRESSIBILITY FACTOR OF CARBON DIOXIDE *
120 REM * USING THE ANALYTIC EQUATION OF STATE DEVELOPED BY IUPAC
130 REM *
140 REM * REFERENCE:
150 REM *  ANGUS,S., ARMSTRONG, B/ AND K. M. DEREUCK
160 REM *  "INTERNATIONAL THERMODYNAMIC TABLES OF THE FLUID STATE, CO2"
170 REM *  PERGAMON PRESS, OXFORD (1976)
180 REM *
190 REM * DESCRIPTION OF VARIABLES:
200 REM *  T: TEMPERATURE IN K
210 REM *  P: PRESSURE IN MPA
220 REM *  RO: DENSITY IN GMOL/ML
230 REM *  B(I,J): PARAMETERS OF THE EQUATION OF STATE
240 REM *  Z: COMPRESSIBILITY FACTOR
250 REM *  Z1,Z2,Z3: VALUES OF Z USED IN THE CONVERGENCE ROUTINE
260 REM *  F1,F2: VALUES OF THE CONVERGENCE FUNCTION
270 REM ************************************************************************
280 :
290 REM * READ IN COEFFICIENTS *
300 :
310 DIM B(9,6)
320 FOR I=0 TO 9
330 ::FOR J=0 TO 6
340 ::::READ B(I,J)
350 ::NEXT J
360 NEXT I
370 DATA -.725854437,-.168332974E1,.259587221,.376945574
380 DATA -.67075537,-.871456126,-.149156928
390 DATA .447869183,.126050691E1,.596957049E1,.154645885E2
400 DATA .194449475E2,.864880497E1,0
410 DATA -.172011999,-.183458178E1,-.461487677E1,-.382121926E1
420 DATA .360171349E1,.492265552E1,0
430 DATA .446304911E-2,-.176300541E1,-.111436705E2,-.278215446E2
440 DATA -.271685720E2,-.642177872E1,0
450 DATA .255491571,.237414246E1,.750925141E1,.661133318E1
460 DATA -.242663210E1,-.257944032E1,0
470 DATA .594667298E-1,.116974683E1,.743706410E1,.150646731E2,.957496845E1,0,
480 DATA -.147960010,-.169233071E1,-.468219937E1,-.313517448E1,0,0,0
490 DATA .136710441E-1,-.100492330,-.163653806E1,-.187082988E1,0,0,0
500 DATA .392284575E-1,.441503812,.886741970,0,0,0,0
510 DATA -.119872087E-1,-.846051949E-1,.464564370E-1,0,0,0,0
```

```
520 :
530 REM * INPUT DESIRED POINT *
540 :
550 REPEAT
560 INPUT "TEMPERATURE (K)";T
570 INPUT "PRESSURE (MPA)";P
580 :
590 REM * INITIAL GUESS *
600 :
610 Z1=.3:Z2=.6
620 :
630 REM * FIND ACTUAL Z
640 :
650 PRINT "ITERATIONS:"
660 PRINT " Z=";Z1
670 Z=Z1:GOSUB 810:F1=Z1-Z
680 REPEAT
690 ::PRINT " Z=";Z2
700 ::Z=Z2:GOSUB 810:F2=Z2-Z
710 ::Z3=(Z2*F1-Z1*F2)/(F1-F2)
720 ::Z1=Z2:Z2=Z3:F1=F2
730 UNTIL ABS(F2)<.000005
740 PRINT "CO2 COMPRESSIBILITY FACTOR =";INT(Z2*1E5+.5)/1E5
750 INPUT "TRY AGAIN (Y/N)";A$
760 UNTIL A$="N"
770 END
780 :
790 REM * SUBROUTINE TO CALCULATE Z FROM IUPAC EQUATION *
800 :
810 RO=P/Z/T/8.314
820 Z=0
830 FOR I=0 TO 9
840 ::FOR J=0 TO 6
850 :::Z=Z+B(I,J)*(304.2/T-1)↑J*(RO/.01063-1)↑I
860 ::NEXT J
870 NEXT I
880 Z=1+Z*RO/.01063
890 RETURN
```

```
100 REM ************************************************************************
110 REM * THIS PROGRAM CALCULATES THE COMPRESSIBILITY FACTOR OF ETHYLENE
120 REM * USING THE HIGH-PRESSURE EQUATION OF STATE DEVELOPED BY IUPAC
130 REM *
140 REM * REFERENCE:
150 REM *  ANGUS, S., ARMSTRONG, B. AND K. M. DEREUCK
160 REM *  "INTERNATIONAL THERMODYNAMIC TABLES OF THE FLUID STATE, ETHYLENE'
170 REM *  PERGAMON PRESS, OXFORD (1972)
180 REM *
190 REM * DESCRIPTION OF VARIABLES:
200 REM *  T: TEMPERATURE IN K
210 REM *  P: PRESSURE IN MPA
220 REM *  RO: DENSITY IN GMOL/ML
230 REM *  B(I,J): PARAMETERS OF THE EQUATION OF STATE
240 REM *  Z: COMPRESSIBILITY FACTOR
250 REM *  Z1,Z2,Z3: VALUES OF Z USED IN THE CONVERGENCE ROUTINE
260 REM *  F1,F2: VALUES OF THE CONVERGENCE FUNCTION
270 REM ************************************************************************
280 REM * READ IN EOS COEFFICIENTS *
290 :
300 DIM B(7,3)
310 FOR I=0 TO 7
320 ::FOR J=0 TO 3
330 ::::READ B(I,J)
340 ::NEXT J
350 NEXT I
360 DATA .2833689,-.3492575E-2,.1232331E-4,-.1320792E-7
370 DATA -.2226079E3,.4728088E1,-.1476258E-1,.1672872E-4
380 DATA -.111773E6,-.6616803E3,.4777931E1,-.6287672E-2
390 DATA -.203427E8,.4064793E6,-.166835E4,.1913838E1
400 DATA .1002623E11,-.9998289E8,.3221877E6,-.3269599E3
410 DATA -.110243E13,.9396738E10,-.2744116E8,.2617866E5
420 DATA .4615094E14,-.3680038E12,.1028783E10,-.9490252E6
430 DATA -.6640149E15,.5165963E13,-.1409796E11,.1271241E8
```

```
440 :
450 REM * INPUT DESIRED POINT *
460 :
470 REPEAT
480 INPUT "PRESSURE (MPA)";P
490 INPUT "TEMPERATURE (T)";T
500 :
510 REM * INITIAL GUESS *
520 :
530 Z1=.3:Z2=.6
540 :
550 REM * FIND Z BY REGULA-FALSI METHOD *
560 :
570 PRINT "ITERATIONS:"
580 PRINT " Z=";Z1
590 Z=Z1:GOSUB 730:F1=Z1-Z
600 REPEAT
610 ::PRINT " Z=";Z2
620 ::Z=Z2:GOSUB 730:F2=Z2-Z
630 ::Z3=(Z2*F1-Z1*F2)/(F1-F2)
640 ::Z1=Z2:Z2=Z3:F1=F2
650 UNTIL ABS(F2)<.000005
660 PRINT "METHYLENE COMPRESSIBILITY FACTOR =";INT(Z2*1E5+.5)/1E5
670 INPUT "TRY AGAIN (Y/N)";A$
680 UNTIL A$="N"
690 END
700 :
710 REM * SUBROUTINE TO CALCULATE Z FROM IUPAC EQUATION *
720 :
730 RO=P/Z/8.314/T
740 Z=0
750 FOR I=0 TO 7
760 ::FOR J=0 TO 3
770 :::Z=Z+B(I,J)*T↑(J-1)*RO↑(I-1)
780 ::NEXT J
790 NEXT I
800 RETURN
```

Appendix B

RAW DATA

The solubility measurements made in this work are given in this appendix. The data is organized into tables of individual isotherms for each supercritical fluid-solute system measured. The data is in the form of peak areas measured on the chromatograph at different system pressures.

The chromatograph operating conditions used to obtain the data are as follows:

- Mobile phase flowrate 2.00 mL/min.
- Column inlet pressure 30.0 MPa.
- Column oven temperature 323.2 K.
- Detector wavelength as given below.
- Detector reference wavelength 430 nm.
- Integrator slope sensitivity setting of 1.0.

The detector wavelength is chosen to yield an acceptable peak response for the substance.

Table 10: Naphthalene-Carbon Dioxide Data at 308.2 K (1).

The detector wavelength is 330 nm. The flow method is used.

Pressure MPa	Peak area	Pressure MPa	Peak Area
10.07	27410	17.41	54820
	27680		55480
	28150		55740
	28660		56330
			55590
12.10	39360		55670
	39550		
	39370	19.58	59860
	40140		61040
			60340
13.96	46960		60850
	47020		
	46930	21.30	63160
	46970		62940
			63860
15.41	51090		63330
	51650		
	51540	22.89	65720
	51850		66240
	51730		66240
			66760

Table 11: Naphthalene-Carbon Dioxide Data at 308.2 K (2).

The detector wavelength is 330 nm. The displacement method is used.

Pressure MPa	Peak Area	Pressure MPa	Peak Area
11.58	36410	17.27	57860
	37300		58040
	34700		56040
	36600		55560
			55680
14.07	47330		
	48490	18.62	58040
	46710		59420
	46560		57770
	47730		59360
15.82	50590	21.37	60560
	50480		61320
	48810		61290
	51010		62430

Table 12: Naphthalene-Carbon Dioxide Data at 318.2 K.

The detector wavelength is 330 nm. The flow method is used.

Pressure MPa	Peak area	Pressure MPa	Peak Area
10.27	16830	17.03	67930
	14770		68670
	15650		68550
	16340		69160
			68490
12.13	30910		
	30830	19.51	79570
	31980		79020
	31690		79620
	31520		80150
13.34	50830	21.96	88110
	51570		88910
	51050		87870
	51460		89190
14.82	57840		
	58270		
	59030		
	58580		

Table 13: Anthracene-Carbon Dioxide Data at 308.2 K.

The detector wavelength is 300 nm. The displacement method is used.

Pressure MPa	Peak Area	Pressure MPa	Peak Area
11.03	75320	16.34	146300
	77490		148300
	74950		152700
	75130		151600
	81460		150400
	80790		151600
12.10	100000	18.62	179700
	95900		173800
	101600		177700
	96300		177600
14.20	125800	21.17	196800
	130700		189500
	124700		188300
	131600		187000
	126400		195800
	128600		

Table 14: Anthracene-Carbon Dioxide Data at 323.2 K.

The detector wavelength is 300 nm. The displacement method is used.

Pressure MPa	Peak Area	Pressure MPa	Peak Area
11.96	36220	17.79	239300
	40910		250600
	35150		248500
	37880		241600
13.82	102400	19.65	283300
	96700		289500
	100600		280300
	103400		285000
	99450		
		21.79	314400
15.93	178800		325800
	170400		322600
	177400		314700
	176900		
	170900	23.86	355100
			350500
			357500
			346100

Table 15: Biphenyl-Carbon Dioxide Data at 308.2 K.

The detector wavelength is 300 nm. The flow method is used.

Pressure MPa	Peak area	Pressure MPa	Peak Area
10.31	238600	18.51	354200
	240200		352000
	236000		359200
	241000		354100
			351300
13.10	270000		
	272800	20.58	386200
	268000		395000
	273100		394500
			391600
14.55	290300		388600
	288600		
	285200	22.10	400600
	291300		393200
			398700
16.06	324200		401400
	318600		
	324200	24.41	425300
	328200		420900
			418600
			416800
			420400

Table 16: Anthracene-Ethylene Data at 308.2 K.

The detector wavelength is 300 nm. The displacement method is used.

Pressure MPa	Peak Area	Pressure MPa	Peak Area
11.31	45450	16.58	119800
	40630		125900
	46150		127300
	41880		123600
	44610		121800
			118200
12.89	70420		
	65570	18.10	145600
	67270		141900
	71940		139100
			145400
14.93	103600		
	99010	20.72	170600
	101300		168500
	95920		173400
	96090		167100
			175800

Table 17: Anthracene-Ethylene Data at 323.2 K.

The detector wavelength is 300 nm. The displacement method is used.

Pressure MPa	Peak Area	Pressure MPa	Peak Area
13.38	63710	19.55	244900
	65390		239600
	59880		243000
	58700		242900
	63320		237400
15.62	150500	21.41	293700
	144300		304300
	151500		293700
	153900		297500
			301700
17.79	209600		
	207900	22.82	338600
	198700		345100
	201300		353700
	209400		345600
	204200		336700

Appendix C

DETERMINATION OF CALIBRATION FACTOR RATIOS

In this Appendix the proportionality constant c_{12} in Equation 9 is determined for naphthalene and anthracene and for anthracene and biphenyl. As mentioned in the Discussion, this is done by direct injection into the chromatograph of solutions of known composition.

The operating conditions of the chromatograph are as follows:

- Mobile phase flowrate 1.00 ml/min.
- Column inlet pressure 30.0 MPa.
- Column oven temperature 323.2 K.
- Detector wavelength as given below.
- Detector reference wavelength 430 nm.
- Integrator slope sensitivity setting 1.0.

C.1 Anthracene-Naphthalene

The peak areas for naphthalene are measured at 330 nm, while those for anthracene are measured at 300 nm. The value of c_{12} determined here must apply to peak areas measured at these wavelengths in order to be usable in this work. Therefore the wavelength of the detector is changed between the elution of the naphthalene and anthracene peaks.

The following solutions of anthracene and naphthalene in approximately 100 mL of acetone are used:

- Solution 1
  - Anthracene 0.13546 g
  - Naphthalene 5.54024 g
- Solution 2
  - Anthracene 0.07323 g
  - Naphthalene 5.71599 g

Table 18 shows the peak areas obtained from several injections of these solutions. The value of c_{12} is obtained from a rearranged form of equation 1

$$c_{12} = (s_2/s_1)(m_1/m_2)(MW_2/MW_1) \qquad (C.1)$$

where m is mass in the solution, MW is molecular weight, and the subscripts 1 and 2 designate anthracene and naphthalene respectively. The calculated values of c_{12} are given in table Table 18. The average value of the 18 measurements of c_{12} is 0.01182, with a standard deviation of .000028. This corresponds to a 95 % confidence interval of 0.001182 + 0.000014.

Table 18: Value of c_{12} for Anthracene (1)-Naphthalene (2).

The detector wavelength is initially 330 nm. After the elution of the naphthalene peak at 1.50 minutes, the detector wavelength is changed to 300 nm. The anthracene peak elutes at 2.12 minutes.

Solution	Injection volume	Peak Area		c_{12}
	10^{-6}L	Naphthalene	Anthracene	x1000
1	10	18460	283800	1.144
		16090	244600	1.157
		18280	277600	1.158
		17560	272400	1.134
		18210	273100	1.172
		18210	271700	1.179
		17390	252600	1.211
		17000	248500	1.203
		17530	259500	1.188
		17210	258000	1.173
		17500	258900	1.189
2	10	24630	189400	1.198
		22180	180400	1.133
		22550	175800	1.182
		23300	174500	1.230
		22250	169900	1.207
	1	4039	30740	1.211
		2846	21810	1.202

C.2 Biphenyl-Anthracene

The following solutions of anthracene and biphenyl in approximately 100 mL of acetone are prepared:

- Solution 1
  - Anthracene 0.07100 g
  - Biphenyl 13.46760 g
- Solution 2
  - Anthracene 0.12227 g
  - Biphenyl 12.49134 g

The peak areas resulting from the injection of these solutions into the chromatograph are shown in Table 19. The table also shows the values of c_{12}, with subscripts 1 and 2 corresponding to biphenyl and anthracene respectively. The average of the 8 measurements of c_{12} is 110.9, with a standard deviation of 1.75. This corresponds to a 95 % confidence interval of 110.9 + 1.46.

Table 19: Value of c_{12} for Biphenyl (1)-Anthracene(2).

The detector wavelength is 300 nm. The biphenyl peak elutes at 1.55 minutes, and the anthracene peak elutes at 2.12 minutes.

Solution	Injection volume	Peak Area		c_{12}
	10^{-6} L	Biphenyl	Anthracene	
1	5	120200	65520	114.0
		145400	72860	109.9
		103100	52480	116.6
2	5	133100	127200	112.8
		139900	129400	109.2
	1	52480	48670	109.5
		56590	52590	109.7

Appendix D

CORRELATION PROGRAM

```
1000 REM ************************************************************************
1010 REM * THIS PROGRAM CALCULATES PREDICTED HEAVY COMPONENT MOLE FRACTIONS
1020 REM * AND THE SUM OF SQUARE RESIDUALS FOR MEASUREMENTS OF THE
1030 REM * SOLUBILITIES OF A SOLID IN A SUPERCRITICAL FLUID.
1040 REM *
1050 REM * THE SOAVE-REDLICH-KWONG EQUATION OF STATE AND ONE PARAMETER
1060 REM * RANDOM MIXING RULES ARE USED.
1070 REM *
1080 REM * NOMENCLATURE:
1090 REM *   SUBSCRIPTS:
1100 REM *     I: COMPONENTS, 1=SUPERCRITICAL SOLVENT, 2=SOLID.
1110 REM *     J: EXPERIMENTAL POINTS
1120 REM *   VARIABLES:
1130 REM *     R: GAS CONSTANT, 8314 J/K/KGMOL
1140 REM *     TC(I): CRITICAL TEMPERATURE IN K.
1150 REM *     PC(I): CRITICAL PRESSURE OF IN PA.
1160 REM *     OM(I): ACENTRIC FACTOR.
1170 REM *     VS: MOLAR VOLUME OF THE SOLID IN M13/KGMOL.
1180 REM *     C1,C2,C3: ANTOINE COEFFICIENTS FOR THE SOLID, PSAT IN PA, T IN K.
1190 REM *     PSAT: VAPOR PRESSURE OF SOLID IN PA.
1200 REM *     T(J): TEMPERATURE IN K.
1210 REM *     P(J): PRESSURE IN PA.
1220 REM *     Y(J): MEASURED MOLE FRACTION OF SOLID.
1230 REM *     YP(J): PREDICTED MOLE FRACTION OF SOLID.
1240 REM *     Y: ASSUMED MOLE FRACTION OF SOLID.
1250 REM *     M(I),AC(I),A(I),B(I): PURE COMPONENT PARAMETERS FOR THE SRK EOS.
1260 REM *     A,B,AA,BB: MIXTURE PARAMETERS FOR THE SRK EOS.
1270 REM *     K: INTERACTION PARAMETER.
1280 REM *     A12: CROSS COEFFICIENT.
1290 REM *     Z: COMPRESSIBILITY FACTOR OF THE MIXTURE.
1300 REM *     PHI: FUGACITY COEFFICIENT OF THE MIXTURE.
1310 REM *     SS: SUM OF SQUARE RESIDUALS.
1320 REM ************************************************************************
```

```
1330 REM ********** INPUT PROPERTIES **********
1340 DIM T(30),P(30),Y(30),YP(30)
1350 R=8314
1360 FOR I=1 TO 2
1370 ::IF I=1 THEN PRINT "FLUID PROPERTIES:":ELSE:PRINT "SOLID PROPERTIES:"
1380 ::INPUT "   CRITICAL TEMPERATURE (K)";TC(I)
1390 ::INPUT "   CRITICAL PRESSURE (MPA)";PC(I):PC(I)=PC(I)*1E6
1400 ::INPUT "   ACENTRIC FACTOR";OM(I)
1410 NEXT I
1420 INPUT "   MOLAR VOLUME (ML/GMOL)";VS:VS=VS*1E-3
1430 PRINT "   ANTOINE COEF. FOR P IN MPA, T IN K"
1440 PRINT "   WHERE PSAT=10↑(C1-C2/(T-C3)):"
1450 INPUT "    C1";C1
1460 INPUT "    C2";C2
1470 INPUT "    C3";C3
1480 REM ********** CALCULATE COMPONENT PARAMETERS **********
1490 FOR I=1 TO 2
1500 ::M(I)=.48+1.574*OM(I)-.176*OM(I)↑2
1510 ::AC(I)=.42747*R↑2*TC(I)↑2/PC(I)
1520 ::B(I)=.08664*R*TC(I)/PC(I)
1530 NEXT I
1540 REM ********** INPUT DATA **********
1550 REPEAT:REM LOOP FOR NEW DATA
1560 PRINT "INPUT DATA"
1570 INPUT "HOW MANY POINTS";N
1580 FOR J=1 TO N
1590 ::REPEAT
1600 ::::PRINT "POINT ";J
1610 ::::INPUT "   TEMPERATURE (K)";T(J)
1620 ::::INPUT "   PRESSURE (MPA)";P(J):P(J)=P(J)*1E6
1630 ::::INPUT "   MOLE FRACTION SOLID";Y(J)
1640 ::::INPUT "   OK (Y/N)";A$
1650 ::UNTIL A$="Y"
1660 NEXT J
1670 REM ********** INPUT K **********
1680 REPEAT:REM LOOP FOR NEW K
1690 INPUT "K";K
```

```
1700 REM ********** MAIN ROUTINE **********
1710 SS=0
1720 PRINT "  T","  P","Y","YP"
1730 FOR J=1 TO N:REM LOOP FOR EACH POINT
1740 ::YP(J)=Y(J):REM ASSUME Y=Y(J)
1750 ::REPEAT:REM LOOP TO CONVERGE YP(J)
1760 ::::Y=YP(J)
1770 ::::REM ********** CALCULATE MIXTURE PARAMETERS **********
1780 ::::FOR I=1 TO 2
1790 ::::::::A(I)=AC(I)*(1+M(I)*(1-(T(J)/TC(I))↑.5))↑2
1800 ::::NEXT I
1810 ::::A12=(A(1)*A(2))↑.5*(1-K)
1820 ::::A=(1-Y)↑2*A(1)+Y↑2*A(2)+2*Y*(1-Y)*A12
1830 ::::B=(1-Y)*B(1)+Y*B(2)
1840 ::::AA=A*P(J)/R↑2/T(J)↑2
1850 ::::BB=B*P(J)/R/T(J)
1860 ::::REM ********** CALCULATE Z **********
1870 ::::Z=.5:REM ASSUME Z=.5
1880 ::::REPEAT:REM LOOP TO CONVERGE Z
1890 ::::::F=Z↑3-Z↑2+Z*(AA-BB-BB↑2)-AA*BB
1900 ::::::DF=3*Z↑2-2*Z+(AA-BB-BB↑2)
1910 ::::::Z=Z-F/DF
1920 ::::UNTIL ABS(F)<5E-6
1930 ::::REM ********** CALCULATE YP **********
1940 ::::P1=-LOG(Z-BB)+B(2)/B*(Z-1)
1950 ::::P2=-AA/BB*(2*(Y*A(2)+(1-Y)*A12)/A-B(2)/B)*LOG(1+BB/Z)
1960 ::::PHI=EXP(P1+P2)
1970 ::::PSAT=10↑(C1-C2/(T(J)-C3))
1980 ::::YP(J)=PSAT/P(J)/PHI*EXP(VS/R/T(J)*(P(J)-PSAT))
1990 ::UNTIL ABS(Y-YP(J))/YP(J)<.00005
2000 ::SS=SS+((Y(J)-YP(J))/YP(J))↑2
2010 ::PRINT T(J),P(J)/1E6,"■■■■";Y(J),"■■■■";INT(1E7*YP(J)+.5)/1E7
2020 NEXT J
2030 PRINT "SUM OF SQUARES=";SS
2040 INPUT "HARD COPY (Y/N)";A$
2050 IF A$="Y" THEN HRDCPY
2060 INPUT "NEW KIJ (Y/N)";A$
2070 UNTIL A$="N"
2080 INPUT "NEW DATA (Y/N)";A$
2090 UNTIL A$="N"
```

BIBLIOGRAPHY

1. Hannay, J. and Hogarth, J., Proc. Roy. Soc. (London), A29, 324 (1879)
2. Tsekhanskaya, Yu. V., Iomtev, M. B. and Mushinka, E. V., Russ. J. Phys. Chem., 38, 1173 (1964).
3. Whitehead, J. C., Coal Mining Process., 16, 9, 84 (1979).
4. Gearhart, J. A. and Garwin, L., Oil Gas J., 74, 63 (1976).
5. Knebel, A. H. and Rhodes, D. E., Proc. 13th Intersoc. Energy Eng. Conf., 438, Society of Automotive Engineers, Warrendale, Pa (1978).
6. Ely, J. F. and Hartwig, J., National Bureau of Standards technical note 1070, Washington (1983).
7. Zosel, K., "Extraction with Supercritical Gases", 1, ed. by Schneider, G. M., Stahl, E. and Wilke, G., Verlag Chimie (1980)
8. Vollbrecht, R., Chem. and Ind., 397 (June 1982).
9. Peaden, P. and Lee, M., J. Liq. Chromatog., 5, 179 (1982).
10. Basta, N., and McQueen, S., Chem. Eng., 14 , (Feb. 4 1985).
11. Randall, L. G., "Chemical Engineering at Supercritical Fluid Conditions", 477, Paulaitis, M. E., Penninger, J. M. L., Gray, R. D. and Davidson, P., editors, Ann Arbor Science, Ann Arbor, Michigan (1983).
12. Scott, R. L. and van Konynenberg, P. H., Disc, Faraday Soc., 49, 87 (1970).

13. van Konynenberg, P. H. and Scott, R. L., Phil. Trans. Roy. Soc. (London), 298, 495 (1980)

14. Chai, C. P., Ph.D. Thesis, University of Delaware (1981).

15. Kurnik, R. T., Holla, S. J. and Reid, R. C., J. Chem. Eng. Data, 26, 47 (1981).

16. van Nieuwenburg, C. J. and van Zon, P. M., Recl. Trav. Chim. Pays-Bas, 54, 129 (1935).

17. Diepen, G. A. M. and Scheffer, P. E. C., J. Am. Chem. Soc., 70, 4085 (1948).

18. van Gunst, C. A., Dissertation, Delft (1950).

19. van Gunst, C. A., Scheffer, F. E. C. and Diepen, G. A. M., J. Phys. Chem., 57, 578 (1953).

20. Ewald, A. J., Jepson, W. B. and Rowlinson, J. S., Discuss. Faraday Soc., 15, 238 (1953).

21. King, A. D. and Robertson, W. W., J. Chem. Phys., 37, 1453 (1962)

22. Tsekhanskaya, Y. V., Iomtev, M. B. and Muskina, E. V., Russ. J. Phys. Chem., 36, 1177 (1962).

23. van Welie, G. S. A. and Diepen, G. A. M., J. Phys. Chem., 67, 755 (1963).

24. Eisenbeiss, J., Southwest Research Institute Final Contract Report DA 18-108-AMC-244(A) (1964).

25. Najour, G. C. and King A. D., J. Chem. Phys., 45, 1915 (1966).

26. Jones, D. and Staehle, R., Editors, "High Pressure Electrochemistry in Aqueous Solutions", 131, National Society of Corrosion Engineers (1973).

27. Johnston, K. P., Thesis, University of Illinois (1979)

28. McHugh, M. A. and Paulaitis, M. E., J. Chem. Eng. Data, 25, 326 (1980).

29. van Leer, R. A. and Paulaitis, M. E., J. Chem. Eng. Data, 25, 257 (1980).

30. Johnston, K. P., Ziger, D. H., and Eckert, C. A., Ind. Chem. Fundam., 21, 191 (1982).

31. Krukonis, V. J., McHugh, M. A. and Seckner, A. J., J. Phys. Chem., 88, 2687 (1984).

32. Cheong, P. L., Masters Thesis, University of Ottawa (1985).

33. McHugh, M. A., Ph.D. Thesis, University of Delaware (1981).

34. Reid, R. C., Prausnitz, J. M. and Sherwood, T. K., "The Properties of Gases and Liquids", 3rd edition, McGraw-Hill, New York (1977).

35. Boublik, T., Fried, V. and Hala, E., "The Vapour Pressures of Pure Substances", Elsevier, Amsterdam (1973).

36. Angus, S., Armstrong, B. and deReuck, K. M., "International Thermodynamic Tables of the Fluid State, Carbon Dioxide", Pergamon Press, Oxford (1976).

37. Angus, S., Armstrong, B. and deReuck, K. M., "International Thermodynamic Tables of the Fluid State, Ethylene, 1972", Pergamon Press, Oxford (1972).

38. Gouw, T. H. and Jentoft, R. E., Adv. Chromatog., 13, 1 (1975).

39. Prins, A., Proc. Acad. Sci. Amsterdam, 17, 1095 (1915).

40. Soave, G., Chem. Eng. Sci., 27, 1197 (1972).